TOXICOLOGY AND APPLIED PHARMACOLOGY **151,** 294–310 (1998)
ARTICLE NO. TO988466

A Pharmacodynamic Analysis of TCDD-Induced Cytochrome P450 Gene Expression in Multiple Tissues: Dose- and Time-Dependent Effects[1]

Michael J. Santostefano,*,[2] Xiaofeng Wang,*,† Vicki M. Richardson,‡ David G. Ross,‡ Michael J. DeVito,‡ and Linda S. Birnbaum‡

Curriculum in Toxicology, University of North Carolina, Chapel Hill, North Carolina 27599-7270; †MGA Software Inc., 200 Baker Avenue, Concord, Massachusetts 01742-2100; and ‡U.S. Environmental Protection Agency, National Health and Environmental Effects Research Laboratory, Experimental Toxicology Division, Pharmacokinetics Branch, Research Triangle Park, North Carolina 27711

Received December 11, 1997; accepted May 7, 1998

A Pharmacodynamic Analysis of TCDD-Induced Cytochrome P450 Gene Expression in Multiple Tissues: Dose- and Time-Dependent Effects. Santostefano, M. J., Wang, X., Richardson, V. M., Ross, D. G., DeVito, M. J., and Birnbaum, L. S. (1998). *Toxicol. Appl. Pharmacol.* **151, 294–310.**

The ability of 2,3,7,8-tetrachlorodibenzo-*p*-dioxin (TCDD, dioxin) to alter gene expression and the demonstration that the induction of CYP1A2 is responsible for hepatic TCDD sequestration suggest that both pharmacokinetic and pharmacodynamic events must be incorporated for a quantitative description of TCDD disposition. In this paper, a biologically based pharmacodynamic (BBPD) model for TCDD-induced biochemical responses in multiple tissues was developed. The parameters responsible for tissue response were estimated simultaneously with a refined physiologically based pharmacokinetic (PBPK) model developed by Wang *et al.* (1997a), by using the time-dependent effects of TCDD on induced CYP1A1/CYP1A2 gene expression in multiple target tissues (liver, lungs, kidneys, and skin) of female Sprague–Dawley rats treated with 10 μg TCDD/kg for 30 min, 1, 3, 8, or 24 h, or 7, 14, or 35 days. This refined BBPD model developed based on the time-course of TCDD-induced CYP1A1/CYP1A2 protein expression, and associated enzymatic activities well described the dose-dependent effects of TCDD on cytochrome P450 protein expression and associated enzyme activities in the multiple tissues of female Sprague–Dawley rats at 3 days following a single exposure to TCDD (0.01–30.0 μg TCDD/kg). This is the first BBPD model to quantitatively describe the time- and dose-dependent effects of TCDD on induced CYP1A1/CYP1A2 protein expression and associated enzyme activities in multiple target tissues for TCDD-induced biochemical responses. © 1998 Academic Press

2,3,7,8-Tetrachlorodibenzo-*p*-dioxin (TCDD, dioxin) belongs to the halogenated aromatic hydrocarbon (HAH) chemical family, which includes polychlorinated dibenzo-*p*-dioxins (PCDDs), dibenzofurans (PCDFs), biphenyls (PCBs), and naphthalenes (PCNs) (Safe, 1986). These compounds share a common Ah receptor (AhR)-mediated mechanism of toxic and biological responses (Safe, 1986; Birnbaum, 1994a; Pohjanvirta and Tuomisto, 1994; Van den Berg *et al.*, 1994; Hankinson, 1995). The most characterized biochemical response associated with TCDD exposure is the induction of CYP1A1 (Whitlock, 1993; Whitlock *et al.*, 1996), which involves the initial interaction of the ligand with the multimeric cytosolic AhR complex (Chen and Perdew, 1994). The ligand:AhR complex undergoes transformation (Denison *et al.*, 1986a; Denison and Yao, 1991), nuclear localization with recruitment of the aryl hydrocarbon receptor nuclear translocase (Arnt) protein (Elferink *et al.*, 1990; Hoffman *et al.*, 1991; Whitelaw *et al.*, 1993), and interaction with dioxin responsive elements (DREs) located within the 5′-flanking regions of TCDD-responsive genes (Gonzalez and Nebert, 1985; Fujisawa-Sehara *et al.*, 1986; Denison *et al.*, 1988a,b). The nuclear ligand:AhR:Arnt:DRE complex results in transcriptional activation of a number of genes, including microsomal monooxygenases (cytochrome P450s), glutathione *S*-transferase, and aldehyde dehydrogenase (Legraverend *et al.*, 1982; Telakowski-Hopkins *et al.*, 1988; Rushmore and Pickett, 1990; Cuthill *et al.*, 1991; Favreau and Pickett, 1991; Savas *et al.*, 1994). Characterization of the mechanism of AhR-mediated responses has resulted

[1] The project described was supported by grant number 1 F32 ES05701-01A1 from the National Institute of Environmental Health Sciences (NIEHS), National Institutes of Health (NIH). Its contents are solely the responsibility of the authors and do not necessarily represent the official views of the NIEHS, NIH. Additional financial support for this research was provided by the U.S. Environmental Protection Agency Cooperative Training Agreement (#T-901915-02) with the University of North Carolina, Chapel Hill, NC 27599-7270 and a gift from the Chemical Manufactures Association. The manuscript has been reviewed in accordance with U.S. Environmental Protection Agency policy and approved for publication; however, it does not necessarily reflect the views of the Agency. Mention of trade names or commercial products does not constitute endorsement or use recommendation.

[2] To whom correspondence should be addressed at the U.S. Environmental Protection Agency (USEPA), National Health and Environmental Effects Research Laboratory (NHEERL), Environmental Toxicology Division (ETD), Pharmacokinetics Branch, Mail Drop-74, Research Triangle Park, NC 27711. Fax: (919) 541-5394; E-mail: santostefano.michael@epamail.epa.gov.

0041-008X/98 $25.00

in the improvement of physiologically based pharmacokinetic (PBPK) and biologically based pharmacodynamic (BBPD) models (King *et al.,* 1983; Leung *et al.,* 1988, 1990a,b; Andersen and Greenlee, 1991; Andersen *et al.,* 1993; Buckley-Kedderis *et al.,* 1993; Kohn *et al.,* 1993; Roth *et al.,* 1994; Buckley, 1995; Kohn *et al.,* 1996).

In a recent article (Wang *et al.,* 1997a), a refined PBPK model incorporating AhR-mediated CYP1A2 gene expression accurately described the distribution of TCDD in multiple tissues (adipose tissue, skin, kidneys, liver, lungs, spleen, and the rest of the body [mainly muscle]) of female Sprague–Dawley rats over time following acute exposure. The PBPK model and parameters obtained were validated using a dose-dependent study for tissue localization in female Sprague–Dawley rats at 3 days following a single exposure to TCDD (0.01–30 μg TCDD/kg). The refined PBPK model also accurately predicted the time course of tissue distribution of TCDD across alternate routes of exposure (oral to iv), as well as between genders of Sprague–Dawley rats (Wang *et al.,* 1997b). Furthermore, the refined PBPK model accurately simulated the time-dependent tissue distribution of TCDD in C57BL/6J mice, as well as the tissue distribution of TCDD in Wistar rats after chronic exposure (Wang *et al.,* 1997b). The approach for this PBPK model demonstrated the importance of experimental design in pharmacokinetic studies, such as using early time points for accurately assigning permeability values and applying the appropriate modeling procedures to reduce the uncertainties in other PBPK models for TCDD by determining unique parameter values.

Recent studies from our laboratory demonstrate that hepatic microsomal sequestration of TCDD does not occur in the CYP1A2(−/−) knockout mouse (Diliberto *et al.,* 1997; Santostefano *et al.,* 1997a). The ability of TCDD to induce CYP1A2 and that CYP1A2 is responsible for the maintenance of high concentrations of TCDD in the liver suggest that both pharmacokinetic and pharmacodynamic events must be incorporated for a quantitative description of TCDD disposition. Therefore, the refined PBPK model for TCDD (Wang *et al.,* 1997a) was coupled to a BBPD model to quantitatively describe the relationship between disposition and tissue response. Previous pharmacodynamic models for TCDD have focused on TCDD-induced responses in only one tissue, the liver (Leung *et al.,* 1988, 1990a; Andersen and Greenlee, 1991; Andersen *et al.,* 1993; Buckley-Kedderis *et al.,* 1993; Kohn *et al.,* 1993; Roth *et al.,* 1994). In order to determine unique parameter values for the PBPK and BBPD models, the effects of TCDD on AhR-mediated cytochrome P450 gene expression were examined in multiple target tissues (liver, lungs, skin, and kidneys) for TCDD-mediated toxicity and biochemical responses (Birnbaum, 1994b; Van den Berg *et al.,* 1994) in female Sprague–Dawley rats treated with 10 μg TCDD/kg for 30 min, 1, 3, 8, or 24 h, or 7, 14, or 35 days. Previously, Roth *et al.,* (1994) described a BBPD model of TCDD tissue localization and TCDD-induced enzyme induction based upon the predicted hepatic CYP1A2 concentration in male rats treated with 0.03–72 μg TCDD/kg. This new BBPD model differs from other models by validating the BBPD model and parameters obtained from the time-course studies in multiple tissues by accurately predicting the dose-dependent effects of TCDD on cytochrome P450 protein expression and associated enzyme activities in the multiple tissues of female Sprague–Dawley rats at 3 days following a single exposure to TCDD (0.01–30.0 μg TCDD/kg).

MATERIALS AND METHODS

Chemicals

2,3,7,8-Tetrachloro[1,6-^{3}H]dibenzo-*p*-dioxin (specific activity of 34.7 Ci/mmol) was purchased from Chemsyn Science Laboratory (Lenexa, KS). Radiochemical purity (≥99%) was verified using both a bioassay involving biliary elimination (Buckley-Kedderis *et al.,* 1991) and reverse-phase high pressure liquid chromatography (Diliberto *et al.,* 1995). Unlabeled TCDD (≥98% stated chemical purity) was obtained from Radian Corp. (Austin, TX). Dosing solutions were prepared by adding a stock of unlabeled TCDD (1 mg/10 ml) in acetone and radiolabeled TCDD (0.91 mCi/ml) in toluene to corn oil. Volatile compounds were removed by evaporation using a Savant Speed-Vac (Savant Instruments Inc., Farmingdale, NY). The TCDD concentrations in the dosing solutions were determined by liquid scintillation counting as described (Santostefano *et al.,* 1996). All other chemicals used in this study were of the highest grade available from commercial sources.

Care and Handling of Animals

Eight-week-old female Sprague–Dawley rats (200–225 g) were purchased from Charles River Laboratories (Raleigh, NC). Rats were maintained at the NHEERL of the USEPA (Research Triangle Park, NC) and followed a diurnal cycle of 12 h of light/dark at an ambient temperature (22 ± 1°C) and relative humidity (55 ± 5%). Each treatment group (5 animals/dose) was randomly assigned and placed in polycarbonate cages, each holding 2–3 animals, with hardwood bedding (Beta Chips, North Eastern Products Inc., Warrensburg, NY). Rats had free access to Purina 5001 Rodent Chow (Ralston Purina Co., St. Louis, MO) and water. Rats were acclimated for 1 week prior to dosing.

Treatment and Tissue Isolation

Five rats were randomly assigned to each time point. Rats were administered a single oral dose of either a corn oil solution containing 10 μg [^{3}H]TCDD/kg body wt or corn oil vehicle alone at 5 ml/kg body wt. At 30 min, 1, 3, 8, or 24 h, or 7, 14, or 35 days after dosing, rats were euthanized by CO_2 asphyxiation (Santostefano *et al.,* 1997b). The liver, lungs, skin, and kidneys were excised, frozen in liquid nitrogen, and stored at −80°C until usage. In a separate experiment, rats received a single oral dose of 0.0 (corn oil), 0.01, 0.1, 0.3, 1.0, 10.0, or 30.0 μg [^{3}H]TCDD/kg at 5 ml/kg body wt and were euthanized by CO_2 asphyxiation 3 days (72 h) after dosing (n = 4 animals/group). The liver, lungs, and kidneys were excised and homogenized in 4 vol (w/v) of ice-cold buffer (250 mM sucrose, 1 mM dithiothreitol, 0.5 mM EDTA, 25 mM KCl, 10 mM HEPES, and 10% [v/v] glycerol pH 7.4) with 20–30 strokes of a Teflon pestle/drill apparatus. The tissue homogenates were centrifuged at 9000*g* for 30 min at 4°C, and the supernatant was frozen in liquid nitrogen and stored at −80°C until usage (Santostefano *et al.,* 1996). The 10.0 μg [^{3}H]TCDD/kg treatment group euthanized by CO_2 asphyxiation 3 days (72 h) after dosing from the dose-response study was also included as a time-point on Figs. 2–5.

CYP1A1/CYP1A2 Protein Measurements

The relative CYP1A1 and CYP1A2 protein concentrations were determined essentially as described (Santostefano *et al.,* 1996). Microsomal proteins were prepared (Diliberto *et al.,* 1995) and quantified using BSA as the standard (Bradford, 1976). Proteins (0.5–20 μg) were resolved by SDS-PAGE using a 10% acrylamide resolving gel and a 4% stacking gel (Laemmli, 1970) and transferred to a 0.2 μm nitrocellulose membrane at 200 mA (1 h) using a Trans-Blot SD Semi Dry Transfer Cell (Biorad Laboratories Inc., Hercules, CA) (Towbin *et al.,* 1979). Membranes were blocked for 1 h at 22°C in Tris-buffered-saline pH 7.5 with 0.05% Tween (TBST), containing 10% nonfat milk. The membrane was probed with a 1:3000 dilution of a rabbit polyclonal antibody against CYP1A1 and CYP1A2 (Human Biological, Phoenix, AZ) in TBST overnight at 4°C. Membranes were probed with a 1:1000 dilution of a secondary goat anti rabbit IgG (H+L)-(human adsorbed) alkaline phosphatase conjugate (Gibco BRL, Gaithersburg, MD) for 1 h at 22°C. CYP1A1 and CYP1A2 proteins were visualized by an alkaline phosphatase reaction for 5–15 min, quantified as optical density units per microgram microsomal protein with a Masterscan densitometer (Billerica, MA), and expressed as fold-induction compared to corn oil-treated animals. The relative CYP1A1 and CYP1A2 protein concentrations, expressed as optical density units per microgram microsomal protein, were linear over the protein concentrations used in the study (data not shown). Molecular weights of CYP1A1 or CYP1A2 immunostained proteins were determined from protein standards (Biorad). All data are represented as the mean ± standard deviation.

Enzymatic Assays

Ethoxyresorufin, methoxyresorufin, and resorufin were purchased from Molecular Probes (Eugene, OR). Microsomal ethoxyresorufin *O*-deethylase (EROD) and methoxyresorufin *O*-demethylase (MROD) activities, markers for CYP1A1 (Pohl and Fouts, 1980) and CYP1A2 (Chaloupka *et al.,* 1995) gene expression, were quantitated spectrofluorimetrically essentially as described (DeVito *et al.,* 1996; Santostefano *et al.,* 1996). Microsomal proteins were prepared (Diliberto *et al.,* 1995) and quantified (Bradford, 1976). The reaction buffer was comprised of 0.1 M KPO_4, 5 mM Mg_2SO_4, and 2 mg bovine serum albumin/ml at pH 7.5. Liver, lung, skin, and kidney microsomes were diluted in 0.1 M KPO_4 (100 μl) to provide linearity of the reaction and then added to the buffer containing 1.5 nM ethoxyresorufin or methoxyresorufin. This reaction mixture, with a total volume of 2.3 ml for the liver samples and 1.0 ml for the nonhepatic samples, was preincubated for 2 min at 37°C. The production of resorufin was started by the addition of 100 μl of β-NADPH (5 mg/ml) and monitored spectrofluorimetrically for 2 min at 37°C with an excitation wavelength of 522 nm and an emission wavelength of 586 nm. The rat liver, lung, skin, and kidney microsomes were analyzed for EROD activity, and the liver microsomes were analyzed for MROD activity. EROD or MROD activity is calculated as pmoles/min/mg microsomal protein and expressed as fold-induction compared to corn oil-treated animals. All data are represented as the mean ± standard deviation.

Model Development

One of the major factors controlling TCDD disposition is CYP1A2 protein expression. Since CYP1A2 is induced by TCDD, a simultaneous PBPK and BBPD model is necessary to describe the tissue disposition of TCDD and the biochemical responses. The PBPK model incorporated with CYP1A2 induction by TCDD in the female Sprague–Dawley rat was reported in detail previously (Wang *et al.,* 1997a). In this paper, a quantitative relationship between TCDD concentration and TCDD-induced cytochrome P450 protein expression and associated enzymatic activities in multiple target tissues was developed based upon receptor theory and AhR-mediated events (Fig. 1).

The induction of CYP1A1 was assumed to result directly from the formation of a TCDD:AhR:DRE complexes (reviewed in Whitlock *et al.,* 1996). A Hill equation was introduced to describe the interaction between the TCDD:AhR complex and DRE binding sites. The change of CYP1A1 with time was described by the model for a stimulation process proposed by Dayneka *et al.* (1993) and Andersen *et al.* (1993). Since EROD activity is a linear biomarker for CYP1A1 (Tritscher *et al.,* 1994; Santostefano *et al.,* 1996), the change of EROD activity with time was assumed to be proportional to the CYP1A1 protein concentration (see Eq. 2 below). Due to the time-dependent process of TCDD:AhR complex formation and subsequent gene activation (Okey *et al.,* 1980; Israel *et al.,* 1985; Denison *et al.,* 1986b), as a first approximation, an apparent delay in the induction of EROD activity (and also CYP1A1 protein expression) was described by a series of biological processes with the holding time, τ (see Eq. 2).

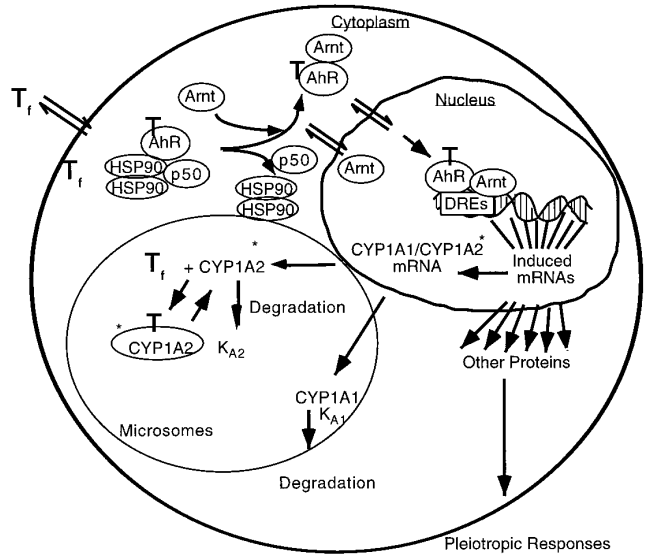

FIG. 1. Proposed AhR-mediated mechanism of the biologically based pharmacodynamic (BBPD) model for cytochrome P450 gene expression by TCDD. This proposed mechanism of TCDD-induced cytochrome P450 gene expression has been extensively reviewed (Safe, 1986; Whitlock, 1993; Birnbaum, 1994a; Hankinson, 1995). Ethoxyresorufin *O*-deethylase (EROD) and methoxyresorufin *O*-demethylase (MROD) activities are markers for CYP1A1 (Pohl and Fouts, 1980) and CYP1A2 (Chaloupka *et al.,* 1995) gene expression, respectively. Concentration of TCDD, T; concentration of free TCDD, T_f; degradation rate of CYP1A1, K_{A1}; CYP1A2, K_{A2}.

Hepatic induction of CYP1A2 was also assumed to result directly from the formation of a TCDD:AhR:DRE complexes (Quattrochi *et al.,* 1994). The Hill equation was introduced to describe the interaction between the TCDD-AhR complex and DRE binding sites, and the change of CYP1A2 with time was described previously (Wang *et al.,* 1997a). As indicated above, a delay of the induction of MROD activity and also CYP1A2 protein expression was also described by a series of biological processes with the holding time, τ (see Eq. 6). The concentration of TCDD specifically bound to either the AhR or CYP1A2 was simplified using the saturable binding equation. As a first approximation, the change of MROD with time was described as a function of CYP1A2 (see Eq. 7 below).

The BBPD model was solved simultaneously with the PBPK model reported previously (Wang *et al.,* 1997a) to obtain the protein induction as well as the enzyme activity induced by TCDD following oral doses. To compare the model predictions of relative CYP1A1 and CYP1A2 protein concentrations and enzymatic activities with the experimental data obtained after exposure to different concentrations of TCDD, we conducted a statistical analysis on the goodness of model prediction to provide information on model prediction with experimental results (Portier and Hoel, 1983, 1984; David, 1978) using the 95% lower and upper bound confidence intervals.

Assuming that the noise (both residual error and inter-individual variability) in the experimental data follows normal distribution, the lower and upper bound of the experimental results at each dose can be obtained, as shown below, when choosing a 95% confidence level:

$$\text{lower bound} = \text{mean value} - t_{0.025} * \text{SD}/(\text{number of animals})^{1/2}$$

$$\text{upper bound} = \text{mean value} + t_{0.025} * \text{SD}/(\text{number of animals})^{1/2},$$

where $t_{0.025} = 3.2$ if $n = 4$; $t_{0.025} = 2.8$ if $n = 5$.

The judgment can also be made based on whether the hypothesis, the experimental data is close to model predictions at each dose, is acceptable or not. Based on the same assumption of normal distribution of experimental samples, the observed value of the test statistic is

$$\text{observed value of the test} = (\text{mean value-model pred.})/\text{SD}/(\text{no. of animals})^{1/2}.$$

The rejection region, with 5% level, is given by 3.2 for a group of 4 animals and 2.8 for a group of 5 animals. If the observed value <3.2 ($n = 4$) or <2.8 ($n = 5$), the hypothesis is acceptable.

Mathematical Expressions of the Model

The mathematical expressions of the PBPK model were given previously (Wang *et al.*, 1997a). The mathematical expressions for CYP1A1 and CYP1A2 induction, as well as EROD and MROD activity, are given below.

CYP1A1 and EROD induction. The change of CYP1A1 with time in the liver was described by the model for a stimulation process proposed by Dayneka *et al.* (1993) and Andersen *et al.* (1993), as shown in Eq. 1.

$$\frac{dC_{\text{A1Li}}}{dt} = K_{0\text{A1Li}}\left(1 + In_{\text{A1Li}}\frac{(C_{\text{Ah-TCDD}})^n}{(IC_{\text{A1}})^n + (C_{\text{Ah-TCDD}})^n}\right) - K_{\text{A1}}C_{\text{A1Li}} \quad (1)$$

at $t = 0$, $C_{\text{A1Li}} = C_{\text{A1BSLi}}$.

Since the concentration of CYP1A1 protein is constant in control animals, $dC_{\text{A1Li}}/dt = 0$. Therefore, $K_{0\text{A1Li}} = K_{\text{A1}}C_{\text{A1BSLi}}$, where C_{A1Li} and C_{A1BSLi} are the total and basal CYP1A1 concentration in the liver, respectively; $K_{0\text{A1Li}}$ represents the zero-order basal rate for CYP1A1 synthesis, and K_{A1} defines the first-order rate constant for CYP1A1 degradation. In_{A1} is the maximum-fold induction rate of CYP1A1 protein expression, $C_{\text{Ah-TCDD}}$ is the concentration of AhR occupied by TCDD, which equals ($\text{Ah}_{\text{T}}C_{\text{Lif}}/K_{\text{DAh}} + C_{\text{Lif}}$), where C_{Lif} is the free concentration of TCDD in the liver, and n is the Hill coefficient for CYP1A1. The delay of CYP1A1 induction by TCDD in the hepatic tissue is described by Eq. 2,

$$\tau\frac{dC_{\text{A1Lij}}}{dt} = C_{\text{A1Li}(j-1)} - C_{\text{A1L}ij}, \quad (2)$$

where τ is the holding time, and j (the number of compartments to simulate the delay in CYP1A1 induction) could be 1, 2, etc., depending on the time of delay of TCDD-induced protein expression and enzyme activity.

Since the hepatic EROD activity was reported as a linear biomarker (Tritscher *et al.*, 1994; Santostefano *et al.*, 1996) for CYP1A1 protein expression, the change of EROD activity with time was then described to be proportional to the change in CYP1A1 protein expression in all tissues as given by Eq. 3.

$$\text{EROD} = \text{Coe}_{\text{A1}}C_{\text{A1}}, \quad (3)$$

where Coe_{A1} is the linear coefficient between CYP1A1 and EROD activity obtained based upon the experimental datas of hepatic CYP1A1 protein expression and EROD activity.

EROD activity was also measured in extrahepatic tissues. CYP1A1 concentration in the extrahepatic tissues were calculated based on Eq. 3, which is $C_{\text{A1k}} = \text{EROD}_k/\text{Coe}_{\text{A1}}$, where, subscript k indicates different extrahepatic tissues. The induction of EROD activity in extrahepatic tissues was described by Eq. 4.

$$\frac{d\text{EROD}_k}{dt} = K_{0\text{ERk}}\left(1 + In_{\text{A1k}}\frac{(C_{\text{Ah-TCDD}})_k^n}{(IC_{\text{A1}})_k^n + (C_{\text{Ah-TCDD}})_k^n}\right) - K_{\text{ER}}\text{EROD}_k, \quad (4)$$

where $K_{0\text{ERk}} = K_{\text{ER}}\text{EROD}_{\text{BSk}}$, $K_{0\text{ERk}}$ is the zero order synthesis rate, K_{ER} is the first order degradation rate, and EROD_{BSk} is the basal level of EROD activity. In addition, without TCDD,

$$\frac{d\text{EROD}_k}{dt} = 0,$$

therefore, $K_{0\text{ERk}} = K_{\text{ER}}\text{EROD}_{\text{BSk}}$.

Hepatic CYP1A2 and MROD induction. The detail for CYP1A2 induction was presented previously (Wang *et al.*, 1997a) and is given by Eq. 5.

$$\frac{dW_{\text{Li}}C_{\text{A2}t}}{dt} = K_{0\text{A2}}\left(1 + In_{\text{A2}}\frac{(C_{\text{Ah - TCDD}})^h}{(IC_{\text{A2}})^h + (C_{\text{Ah - TCDD}})^h} - K_{\text{A2}}C_{\text{A2t}}\right)W_{\text{Li}} \quad (5)$$

at $t = 0$, $C_{\text{A2}t} = C_{\text{A2BS}}$.

Since the concentration of CYP1A2 protein is constant in control animals, $dW_{\text{Li}}C_{\text{A2}t}/dt = 0$.Therefore, $K_{0\text{A2}} = K_{\text{A2}}C_{\text{A2BS}}$, where $C_{\text{A2}t}$ and C_{A2BS} are the total and basal CYP1A2 concentrations, respectively, $K_{0\text{A2}}$ represents the zero-order basal rate for CYP1A2 synthesis, and K_{A2} defines the first-order rate constant for CYP1A2 degradation. In_{A2} is the maximum fold induction rate for CYP1A2 protein expression, and h is the Hill coefficient for CYP1A2. $C_{\text{Ah-TCDD}}$, which equals $\text{Ah}_{\text{Li}}C_{\text{Lif}}/K_{\text{DAh}} + C_{\text{Lif}}$, is the concentration of AhR occupied by TCDD. The delay of CYP1A2 induction is described by Eq. 6,

$$\tau\frac{dC_{\text{A2}tj}}{dt} = C_{\text{A2}t(j-1)} - C_{\text{A2}tj}, \quad (6)$$

where τ is the holding time, and $j = 1,2$, etc., depending on the time of delay in TCDD-induced protein expression and enzyme activity.

The change of MROD with time was described as a function of CYP1A2,

$$\frac{d\text{MROD}}{dt} = In_{\text{MR}}C_{\text{A2}t} - K_3\text{MROD} \quad (7)$$

at $t = 0$, $\text{MROD} = \text{MROD}_{\text{BS}}$ where In_{MR} is the first-order synthesis rate of MROD activity, K_3 defines the first-order rate constant for MROD degradation, and MROD_{BS} is the basal MROD activity. Without TCDD, $d\text{MROD}/dt = 0$, therefore, $In_{\text{MR}}C_{\text{A2BS}} = K_{\text{MR}}\text{MROD}_{\text{BS}}$.

Parameter Estimation

The dissociation constant of TCDD bound to the AhR, the maximum CYP1A2 induction rate, the degradation rate constant of CYP1A2, and the Hill coefficient, as well as dissociation constant of TCDD binding to CYP1A2, were obtained previously (Wang *et al.*, 1997a). τ and j were determined by fitting the model to the time-course data for CYP1A1 and CYP1A2 protein expression, as well as the hepatic tissue concentration of TCDD. The parameters of MROD activity induction and degradation were obtained by fitting Eq. 7 to the experimental data of the time course of MROD activity.

As an initial first-approximation, the degradation rate constant of CYP1A1 in different tissues was assumed to be the same. The maximum induction rates of CYP1A1 in different tissues were considered a result of the different concentrations of AhR, as well as the interaction with DNA. The maximum fold of CYP1A1 induction rate, the degradation rate constant of CYP1A1, the interaction of TCDD: AhR with DNA, and the Hill coefficient for CYP1A1 were obtained by fitting the

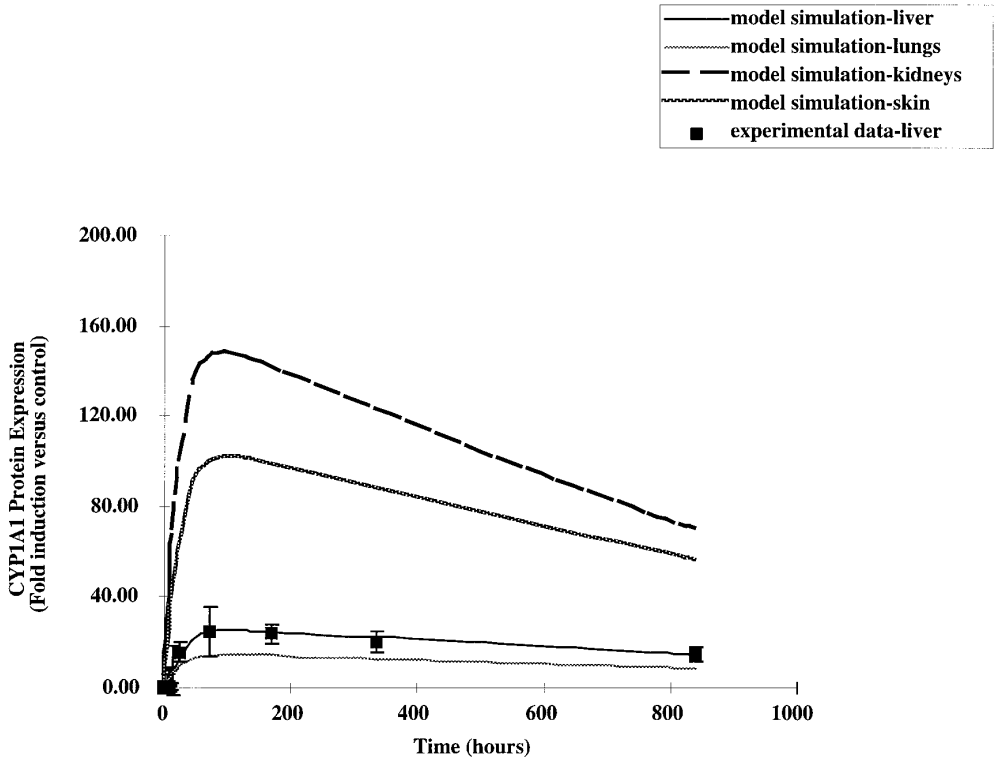

FIG. 2. Time-dependent effects of TCDD on CYP1A1 protein expression in the liver, lungs, kidneys, and skin of female Sprague–Dawley rats treated with 10 μg TCDD/kg with BBPD model simulation. The hepatic CYP1A1 protein concentration was quantitated as described (Santostefano *et al.*, 1996) and expressed as fold induction compared to control animals. These data have been adapted from Santostefano *et al.* (1997b). All symbols were obtained from TCDD-treated animals as described in Materials and Methods. Solid and broken lines were derived from the BBPD model simulation of the experimental data. ■, hepatic CYP1A1 protein concentration. Data are presented as mean ± SD (n = 4–5).

model to the CYP1A1 time-course data. In the hepatic tissue, τ and j are determined by fitting the model to CYP1A1 time-course data.

Model simulations were conducted using ACSL TOX (MGA Software Inc., Concord, MA).

RESULTS

The objectives of this study were 2-fold: (1) to develop a BBPD model to quantitatively describe the time-dependent effects of TCDD on cytochrome P450 protein expression and associated enzyme induction in multiple target tissues (liver, lungs, skin, and kidneys) of female Sprague–Dawley rats and (2) to validate the BBPD model and parameters obtained from the time-course studies in multiple tissues with the dose-dependent effects of TCDD on cytochrome P450 protein expression and associated enzyme activities in the multiple tissues of female Sprague–Dawley rats at 3 days following a single exposure to TCDD (0.01–30.0 μg TCDD/kg).

Time-Dependent Expression of CYP1A1 and CYP1A2 Proteins in the Liver

Figures 2 and 3 illustrate the time-dependent effects of TCDD on CYP1A1 and CYP1A2 protein expression in the liver of female Sprague–Dawley rats treated with 10 μg TCDD/kg. TCDD-induced hepatic CYP1A1 (~56 kDa) and CYP1A2 (~54 kDa) protein expression was increased approximately 16- and 6-fold, respectively, relative to control animals 24 h after TCDD administration. Maximal TCDD-induced CYP1A1 and CYP1A2 protein expression was observed 72 h (3 days) after TCDD treatment. This induction was maintained at 14 days with a slight decrease by Day 35.

Based on the above data (Fig. 2), a BBPD model (Fig. 1) was developed to analyze the time-dependent effects of TCDD on CYP1A1 protein expression in the liver. The induction of CYP1A1 was assumed to result directly from the formation of a TCDD:AhR:DRE complex described by the model for a stimulation process (see Materials and Methods section). The dissociation constant of TCDD bound to the AhR (0.1 nM) was obtained from previous studies (Wang *et al.*, 1997a). The Hill coefficient, which describes the interaction of the TCDD:AhR complex with DNA sites responsible for CYP1A1 protein expression, was determined by fitting Eq. 1 to the time-course experimental data for hepatic CYP1A1 protein expression by TCDD (Fig. 2). The estimated parameter values are given in Table 1. These parameters accurately simulated the time-dependent effects of TCDD on CYP1A1 protein expression in the liver using the BBPD model (Fig. 2).

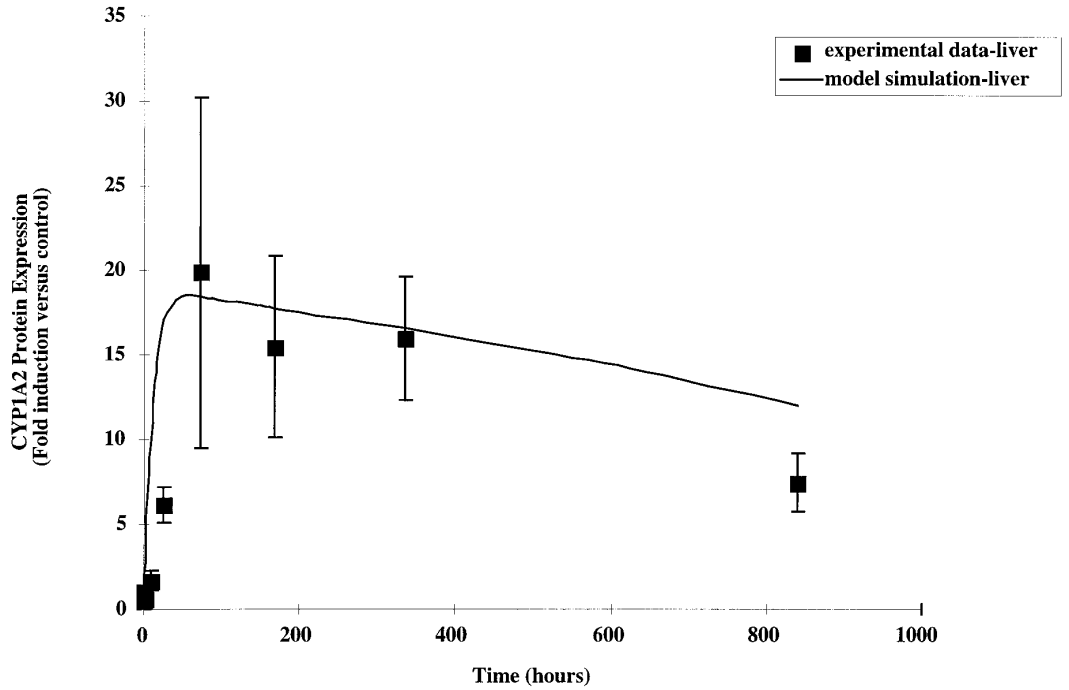

FIG. 3. Time-dependent effects of TCDD on CYP1A2 protein expression in the liver of female Sprague–Dawley rats treated with 10 μg TCDD/kg with BBPD model simulation. The hepatic CYP1A2 protein concentration was quantitated as described (Santostefano *et al.,* 1996) and expressed as fold induction compared to control animals. These data have been adapted from Santostefano *et al.* (1997b). All symbols were obtained from TCDD-treated animals as described in Materials and Methods. The solid line was derived from the BBPD model simulation of the experimental data. ■, hepatic CYP1A2 protein concentration. Data are presented as mean ± SD (n = 4–5).

The induction of CYP1A2 was also assumed to result directly from the formation of TCDD:AhR:DRE complexes described by the model for a stimulation process (see Materials and Methods section). The dissociation constant of TCDD binding to CYP1A2 (130 nM), the basal CYP1A2 concentration, the maximum fold induction rate, and the first order degradation rate constant for CYP1A2, as well as the Hill coefficient, which describes the interaction between TCDD: AhR complex and DNA sites responsible for CYP1A2 protein expression, were determined from the previous study (Wang *et al.,* 1997a) by combining time-course tissue distribution data with CYP1A2 time-course data. The delay for CYP1A2 induction was obtained by fitting Eq. 6 to the CYP1A2 experimental data while simultaneously fitting the TCDD tissue distribution in the liver. The estimated values for these parameters are shown in Table 1. With these parameters, the time course of CYP1A2 protein expression in the liver after exposure to TCDD was well described (Fig. 3).

Time-Dependent Expression of EROD and MROD Activities in the Liver

Figure 4 shows both the experimental results and model simulation of the time-dependent effects of TCDD on EROD activity in the liver of female Sprague–Dawley rats exposed to 10 μg TCDD/kg. Constitutive hepatic EROD activity was 343.0 pmol/min/mg microsomal protein. Three days (72 h) after TCDD treatment, maximal TCDD-induced hepatic EROD activity was approximately 36-fold compared to control animals, which was followed by a slight time-dependent decrease in EROD activity by day 35 (Fig. 4).

The BBPD model accurately described the time-dependent effects of TCDD on hepatic EROD activity up to 35 days after exposure within the experimental error (Fig. 4). Since EROD has been demonstrated as a linear biomarker for CYP1A1 in all tissues (Tritscher *et al.,* 1994; Santostefano *et al.,* 1996), the linear coefficient (Table 1) between CYP1A1 protein expression and EROD activity was determined by fitting Eq. 3 to EROD activity and CYP1A1 protein expression. This value is related to the units used for both enzyme activity (pmoles per minute per milligrams microsomal protein) and CYP1A1 protein expression (optical density units per microgram microsomal protein). The results are shown in Table 1.

Figure 5 shows the time-dependent effects of TCDD on MROD activity in the liver of female Sprague–Dawley rats exposed to 10 μg TCDD/kg. Constitutive MROD activity was 74.0 pmol/min/mg microsomal protein. Seven days (168 h) after TCDD treatment, maximal TCDD-induced MROD activity, approximately 21-fold compared to control animals, was found (Fig. 5). The increase in TCDD-induced MROD activity

TABLE 1
Results of Parameter Estimation

Model parameters	Abbreviation	Values	Parameter estimation
Liver Weight (g)	W_{Li}	9.05	Measured
Lungs Weight (g)	W_{Lu}	0.81	Measured
Skin Weight (g)	W_S	45.80	Measured
Kidneys Weight (g)	W_K	1.64	Measured
CYP1A2[a]			
Basal concentration (nmol/g)	C_{A2BS}	1.6	Buckley-Kedderis, (1991), Weber *et al.*, 1993
Degradation rate (h^{-1})	K_{A2}	0.1	Wang *et al.*, 1997a
Maximum induction fold for CYP1A2	In_{A2}	600.0	Wang *et al.*, 1997a
TCDD:Ah:DNA to induce CYP1A2 (nM)	IC_{A2}	130.0	Wang *et al.*, 1997a
TCDD:CYP1A2 (nM)	K_{DA2}	35.0	Wang *et al.*, 1997a
Hill coefficient	h	0.6	Wang *et al.*, 1997a
No. compartments to simulate delay	j	3	Estimated from BBPD
Holding time for delay (h)	τ	2	Estimated from BBPD
CYP1A1[a]			
TCDD:Ah:DNA (CYP1A1) (nM)	IC_{A1}	10	(Tritscher *et al.*, 1992) and adjusted from BBPD model
Hill coefficient (nM)	n	1	Wang *et al.*, 1997a
Linear coefficient between EROD & CYP1A1 (EROD activity/CYP1A1 protein)	Coe_{A1}	1500	Estimated from BBPD model
No. compartments to simulate delay	j	3	Estimated from BBPD
Holding time for delay (h)	τ	2 (Li) 1 (Lu) 1 (K) 0.2 (S)	Estimated from BBPD
EROD activity[b]			
Basal EROD activity (liver)	$EROD_{BsLi}$	343	Constitutive EROD activity
Basal EROD activity (lungs)	$EROD_{BsLu}$	11.0	Constitutive EROD activity
Basal EROD activity (kidneys)	$EROD_{BsK}$	6.0	Constitutive EROD activity
Basal EROD activity (skin)	$EROD_{BsS}$	0.2	Constitutive EROD activity
Degradation rate (h^{-1})	K_{ER}	0.04	Estimated from BBPD model
Maximum EROD induction rate (activity/h) in the liver	In_{ERLi}	900	Estimated from BBPD model
Maximum EROD induction rate (activity/h) in the lungs	In_{ERLu}	500	Estimated from BBPD model
Maximum EROD induction rate (activity/h) in the kidneys	In_{ERK}	8000	Estimated from BBPD model
Maximum EROD induction rate (activity/h) in the skin	In_{ERS}	22000	Estimated from BBPD model
MROD[b]			
Basal activity (liver)	$MROD_{BS}$	74.3	Constitutive MROD activity
Synthesis rate (activity/h)	IN_{MR}	3.7	Estimated from BBPD model
Degradation rate (h^{-1})	K_3	0.08	Estimated from BBPD model
AhR			
TCDD:AhR (nM)	K_{DAh}	0.1	Wang *et al.*, 1997a

[a] Optical density per microgram microsomal protein.
[b] Picomoles per minute per milligram microsomal protein.

remained elevated for 840 h (35 days) after TCDD exposure (Fig. 5).

Parameters responsible for MROD induction, such as the basal MROD activity, the first-order synthesis rate, and degradation rate constant for MROD activity, were determined by fitting Eq. 7 to the above data (Fig. 5). The model simulation well represents the time-dependent change in MROD activity in the liver up to 35 days after exposure to TCDD (Fig. 5).

Time-Dependent Expression of CYP1A1 Protein and EROD Activity in Extrahepatic Tissues

Figure 4 shows both the experimental results and model simulation of the time-dependent effects of TCDD on EROD activity in the lungs, kidneys, and skin of female Sprague–Dawley rats exposed to 10 μg TCDD/kg. Constitutive EROD activity was 11.0, 6.0, and 0.2 pmol/min/mg microsomal pro-

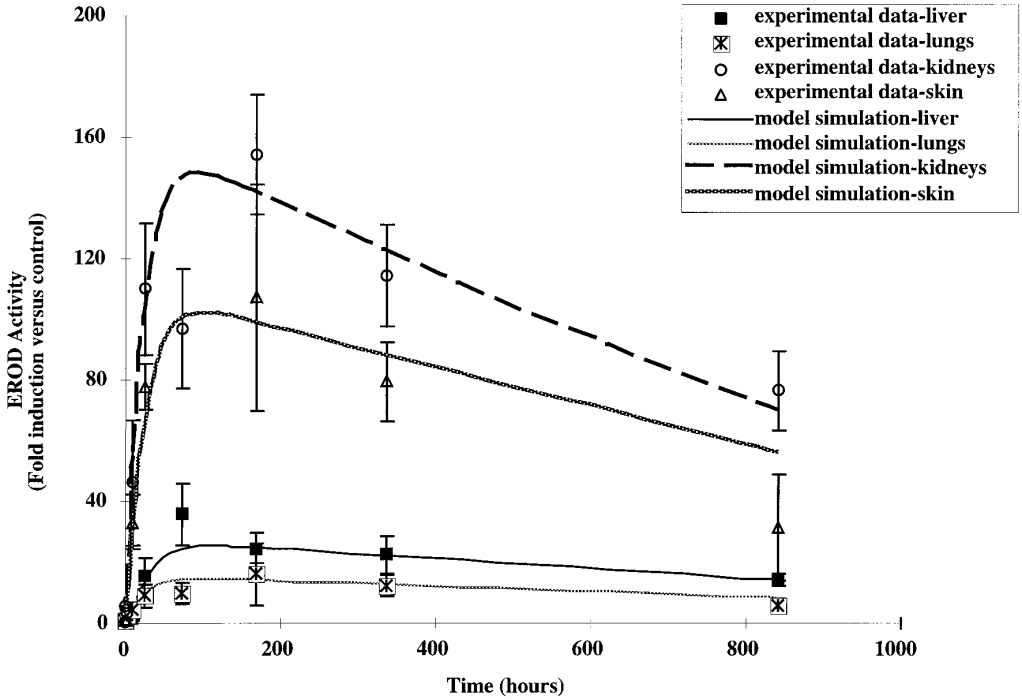

FIG. 4. Time-dependent effects of TCDD on EROD activity in the liver, lungs, kidneys, and skin of female Sprague–Dawley rats treated with 10 μg TCDD/kg with BBPD model simulation. EROD activity determined from 0–35 days. EROD activity was quantitated spectrofluorimetrically as described (DeVito *et al.*, 1996). EROD activity is expressed as fold induction compared to control animals. All symbols were obtained from TCDD-treated animals as described in Materials and Methods. Solid and broken lines were derived from the BBPD model simulation of the experimental data. ■, EROD activity in liver; ○, EROD activity in kidneys; x, EROD activity in lungs; ◇, EROD activity in skin. Data are presented as mean ± SD (n = 4–5).

tein in the lungs, kidneys, and skin, respectively. Seven days (168 h) after TCDD treatment, maximal TCDD-induced EROD activity was found in all tissues, which was followed by a time-dependent decrease in EROD activity (Fig. 4).

The zero order synthesis rate, the first order degradation rate constant, and the maximum fold induction rate for EROD activity (pmol/min/mg microsomal protein) in extrahepatic tissues were estimated by fitting Eq. 4 to the time-course experimental data (shown in Fig. 4). The model simulation well represents the time-dependent effects of TCDD on EROD activity in extrahepatic tissues up to 35 days after exposure (Fig. 4).

The linear coefficient (Table 1) between EROD and CYP1A1 obtained from the liver was then employed to estimate the CYP1A1 concentration in the extrahepatic tissues based upon the EROD activity in the extrahepatic tissues.[3] The results are given in Fig. 2. The BBPD model predicts that TCDD induces a similar change in the time-course expression of CYP1A1 protein in the lungs, kidneys, and skin as in the liver (Fig. 2).

[3] Because of the detection limits of the CYP1A1 protein assay, the CYP1A1 protein concentration was not determined in extrahepatic tissues.

Dose-Dependent Expression of Cytochrome 450 Proteins

Figures 6 and 7 illustrate the dose-dependent effects of TCDD on CYP1A1 and CYP1A2 protein expression in the liver of female Sprague–Dawley rats at 3 days following a single exposure to TCDD (0.01–30.0 μg TCDD/kg). TCDD induced hepatic CYP1A1 protein in rats treated with 0.3 μg TCDD/kg or higher compared to corn oil-treated animals (Fig. 6). TCDD induced hepatic CYP1A2 protein in rats treated with 1.0 μg TCDD/kg or higher compared to corn oil-treated animals (Fig. 7). Maximum induction of hepatic CYP1A1 or CYP1A2 protein expression, approximately 25- and 28-fold vs control, was observed at 10.0 μg TCDD/kg.

The parameters obtained from the time-course effects of TCDD on CYP1A1 and CYP1A2 protein expression (shown in Table 1) were used to describe the effect of dose of TCDD on hepatic CYP1A1 and CYP1A2 protein expression. Statistical analysis on the goodness of model prediction of CYP1A1 and CYP1A2 protein expression and enzymatic activities after exposure to different concentrations of TCDD, based upon the BBPD model and parameters in Table 1 developed from the time-course of TCDD-induced CYP1A1/CYP1A2 protein expression and associated enzymatic activities, are not statistically different from the experimental results for a majority of the data points. The BBPD parameters predicted the dose-

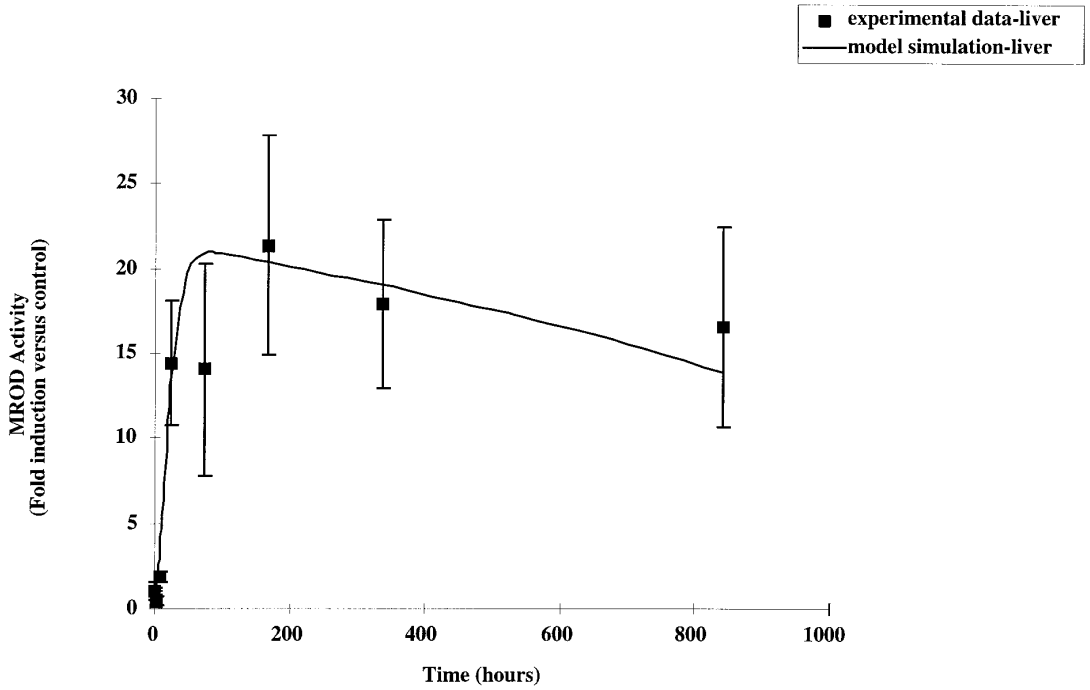

FIG. 5. Time-dependent effects of TCDD on MROD activity in the liver of female Sprague–Dawley rats treated with 10 μg TCDD/kg with BBPD model simulation. MROD activity was quantitated spectrofluorimetrically as described (DeVito *et al.*, 1996). MROD activity is expressed as fold induction compared to control animals. All symbols were obtained from TCDD-treated animals as described in Materials and Methods. The solid line was derived from the BBPD model simulation of the experimental data. ■, MROD activity in liver. Data are presented as mean ± SD (n = 4–5).

dependent effects of TCDD on CYP1A1 and protein expression in the liver well (Fig. 6). These parameters were utilized to simulate the dose-dependent effects of TCDD on CYP1A1 protein expression in the kidneys and skin.[3] The model predicted that TCDD caused a similar dose-dependent increase in CYP1A1 protein expression in the lungs, kidneys, and skin, as in the liver (Fig. 6). Using 0.02 optical density units/mg microsomal protein as a limit of detection for hepatic CYP1A1 protein expression in control animals, recent experiments have confirmed that the BBPD model and model parameters accurately predicted the dose-dependent increase in TCDD-induced CYP1A1 protein expression in the lungs (Fig. 6). Analysis of TCDD-induced CYP1A2 protein expression by the BBPD model suggests that these parameters (Table 1) predict the dose-dependent change in the CYP1A2 protein expression by TCDD in the range of 0.01–30.0 μg TCDD/kg (Fig. 7).

Dose-Dependent Expression of EROD and MROD Activities

Figure 8 shows the dose-dependent effects of TCDD on EROD activity in the liver, lungs, and kidneys of female Sprague–Dawley rats at 3 days following a single exposure to TCDD (0.01–30.0 μg TCDD/kg). Constitutive EROD activity was 490.0, 3.0, and 2.0 pmoles/min/mg microsomal protein in the liver, lungs, and kidneys, respectively. In all tissues examined, a dose-dependent increase in TCDD-induced EROD activity was observed in the liver, lungs, and kidneys of rats treated with different doses (0.01–30.0 μg TCDD/kg). Female Sprague–Dawley rats treated with 30 μg TCDD/kg exhibited a maximal fold induction of TCDD-induced EROD activity of approximately 40-, 16-, and 100-fold vs control animals in the liver, lungs, and kidneys, respectively. Figure 9 shows the dose-dependent increase in MROD activity in the liver of female Sprague–Dawley rats at 3 days following a single exposure to TCDD (0.01–30.0 μg TCDD/kg). Constitutive MROD activity was 171.0 pmol/min/mg microsomal protein. Both TCDD-induced hepatic EROD and MROD induction showed a saturable relationship (Figs. 8 and 9).

Using the model parameters obtained from the time-dependent effects of TCDD on EROD activity in the liver, skin, lungs, and kidneys (shown in Table 1), the BBPD model was employed to predict the dose-dependent effects of TCDD on EROD activity in the liver, lungs, skin, and kidneys. Statistical analysis on the goodness of model prediction of CYP1A1 and CYP1A2 protein expression and enzymatic activities after exposure to different concentrations of TCDD based upon the BBPD model and parameters in Table 1 developed from the time-course of TCDD-induced CYP1A1/CYP1A2 protein expression and associated enzymatic activities was not statistically different from the experimental results for a majority of the data points. Figure 8 shows that the model predicted well for the dose-dependent effects of TCDD on EROD in the liver, lungs, and kidneys and simulated TCDD-induced EROD ac-

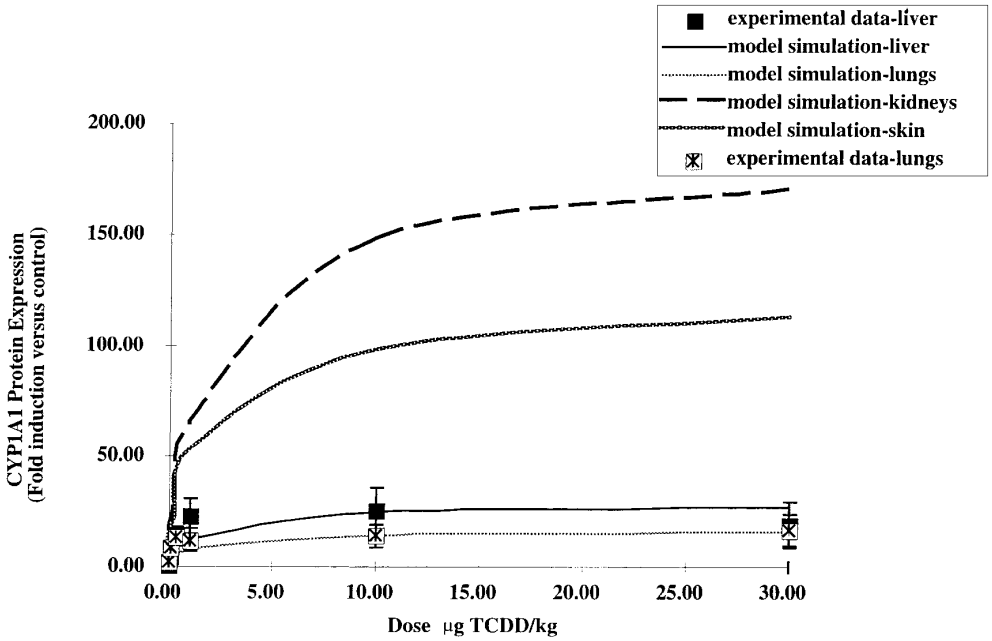

FIG. 6. Dose-dependent effects of TCDD on CYP1A1 protein expression in the liver, lungs, kidneys, and skin of female Sprague–Dawley rats with BBPD model simulation. The hepatic CYP1A1 protein concentration was quantitated as described (Santostefano *et al.,* 1996) and expressed as fold induction compared to control animals. These data have been adapted from Santostefano *et al.* (1997b). All symbols were obtained from TCDD-treated animals as described in Materials and Methods. Solid and broken lines were derived from the BBPD model simulation of the experimental data. ■, hepatic CYP1A1 protein concentration; x, CYP1A1 protein concentration in lungs. Data are presented as mean ± SD (n = 4–5).

tivity in the skin.[4] The BBPD model overpredicts the dose-dependent increase in EROD activity in the kidneys and lungs (Fig. 8). The model simulation suggested that TCDD caused a similar dose-dependent change in EROD activity in the skin as observed in the liver, lungs, and kidneys (Fig. 8). The parameters responsible for MROD induction (Table 1) obtained from the time-dependent effects of TCDD on MROD activity in the liver were also used to predict the dose-dependent effects of TCDD on MROD activity. The model simulation overpredicts the dose-dependent effects of TCDD on MROD activity in the liver (Fig. 9).

DISCUSSION

TCDD induces mixed function oxidase activities catalyzed by cytochrome P450 isozymes (Poland and Glover, 1974). Among the most characterized biochemical responses induced by TCDD and related compounds through an AhR-dependent mechanism are CYP1A1, CYP1A2, and CYP1B1 (Safe, 1986; Whitlock, 1993; Birnbaum, 1994a; Hankinson, 1995). These cytochrome P450s are a class of heme-containing proteins which oxidize endogenous and exogenous substrates into readily metabolized hydrophilic products (Guengerich, 1990). CYP1A2 not only functions as a phase I enzyme but was hypothesized to be responsible for the hepatic sequestration of TCDD and related compounds (Voorman and Aust, 1987, 1989; Poland *et al.,* 1989a,b; Buckley-Kedderis *et al.,* 1993; Santostefano *et al.,* 1996, 1997a; Diliberto *et al.,* 1997). Recent studies using CYP1A2 knock-out mice have clearly demonstrated that CYP1A2 is the binding protein responsible for hepatic sequestration of TCDD and related compounds (Diliberto *et al.,* 1997; Santostefano *et al.,* 1997a). For example, Diliberto *et al.,* (1997) showed no sequestration of TCDD or 2,3,4,7,8-pentachlorodibenzofuran (a potent AhR agonist) in the liver of mice lacking a functional CYP1A2 gene. In addition, Santostefano *et al.,* (1997a) demonstrated that hepatic microsomal localization of TCDD is reduced in the CYP1A2 −/− mouse. Therefore, the ability of TCDD to induce CYP1A2, the TCDD-binding protein, appears to be the mechanism for maintenance of high concentrations of TCDD in the liver, suggesting that both pharmacokinetic and pharmacodynamic events must be incorporated for a quantitative description of TCDD disposition.

The BBPD model was developed based on the AhR-mediated mechanism of cytochrome P450 gene expression and associated enzyme induction by TCDD (Fig. 1). Previous pharmacodynamic studies focused on TCDD-induced biochemical responses in the liver (Andersen *et al.,* 1993; Kohn *et al.,* 1993; Portier *et al.,* 1993; Roth *et al.,* 1994) with CYP1A1 and CYP1A2 induction assumed to result directly from formation

[4] Skin EROD was not determined experimentally since the tissue obtained from the TCDD dose-response study was frozen prior to homogenization (see Materials and Methods).

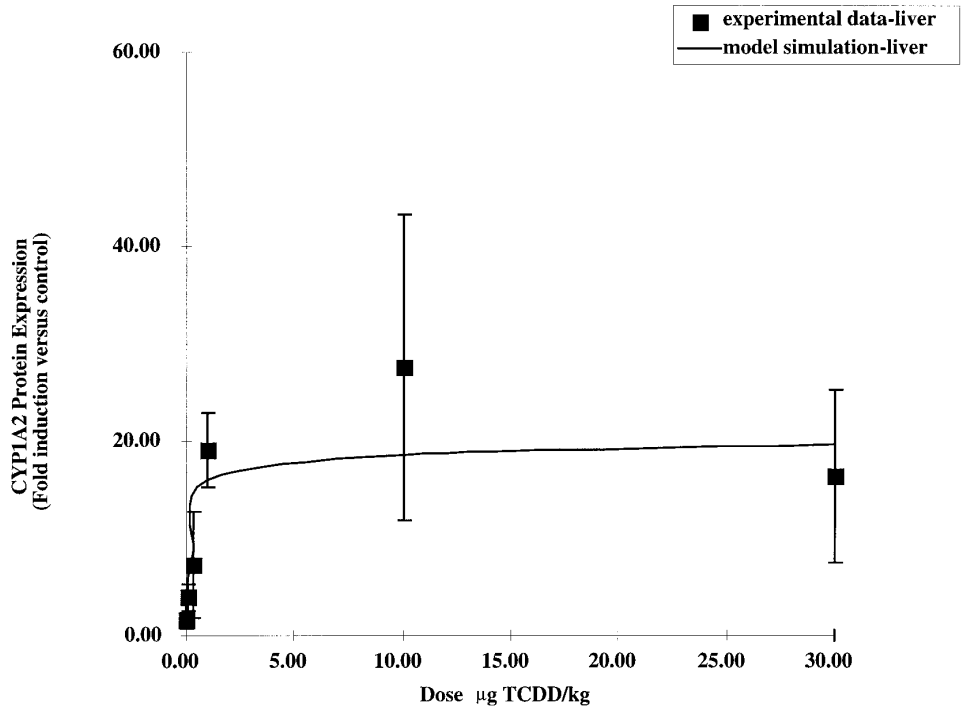

FIG. 7. Dose-dependent effects of TCDD on CYP1A2 protein expression in the liver of female Sprague–Dawley rats with BBPD model simulation. The hepatic CYP1A2 protein concentration was quantitated as described (Santostefano *et al.,* 1996) and expressed as fold induction compared to control animals. These data have been adapted from Santostefano *et al.* (1997b). All symbols were obtained from TCDD-treated animals as described in Materials and Methods. The solid line was derived from the BBPD model simulation of the experimental data. ■, hepatic CYP1A2 protein concentration. Data are presented as mean ± SD (n = 4–5).

of TCDD:AhR:DRE complexes (Quattrochi *et al.,* 1994; Whitlock *et al.,* 1996). Many studies have proposed that the binding of TCDD to induced CYP1A2 is the major reason for liver sequestration of the chemical (Santostefano *et al.,* 1996 and references therein). However, previous models and parameters (Leung *et al.,* 1988, 1990a; Andersen, *et al.,* 1993) were estimated based upon a lack of information on CYP1A2 induction at that time. Therefore, it is also unlikely that those parameters obtained from previous studies can be determined uniquely. For example, Wang *et al.* (1997a) demonstrated that by adjusting parameter values, such as the fold induction of CYP1A2 and the dissociation constant for the interaction between CYP1A2 and TCDD, similar fitting results for tissue distribution can be achieved. Kohn and coworkers (1993) assumed that both hepatic CYP1A1 and CYP1A2 induction were kinetic processes, and the parameters related to the synthesis and degradation of these cytochrone P450s, as well as the Hill coefficient, were estimated based on chronic studies. In our previous (Wang *et al.,* 1997a) and current studies, we extended the previous pharmacodynamic models by determining the parameter values based on time course of CYP1A1 and CYP1A2 responses in multiple tissues after acute exposure to TCDD and then validated the model with data obtained from dose-dependent studies. The parameter values obtained from the present study (Table 1) are different from other reported BBPD parameter values for TCDD (Leung *et al.,* 1988, 1990a; Andersen *et al.,* 1993; Kohn *et al.,* 1993; Roth *et al.,* 1994), as previously described by Wang *et al.* (1997a). For example, previous studies by Roth *et al.* (1994) described a BBPD model of TCDD tissue localization and TCDD-induced enzyme induction based upon the predicted hepatic CYP1A2 concentration in male rats treated with 0.03–72 μg TCDD/kg. In this study, the new BBPD model differs from other models in that the BBPD model obtained from the time-course studies of measured CYP1A1 and CYP1A2 protein concentrations and associated enzymatic activities in multiple tissues was validated by accurately predicting the dose-dependent effects of TCDD on cytochrome P450 protein expression and associated enzyme activities in the multiple tissues of female Sprague–Dawley rats at 3 days following a single exposure to TCDD (0.01–30.0 μg TCDD/kg). Another reason for the differences in BBPD parameter estimation between the studies may be due to the limited quantitative information on the biochemical process of AhR-dependent gene activation by TCDD and use of different assumptions in previous studies (Leung *et al.,* 1988, 1990a; Andersen *et al.,* 1993; Kohn *et al.,* 1993; Roth *et al.,* 1994) as detailed previously by Wang and coworkers (1997a). Therefore, unique numerical results may not be able to be obtained (Wang *et al.,* 1997a). However, the maximum hepatic EROD induction rate as observed in this study (Table

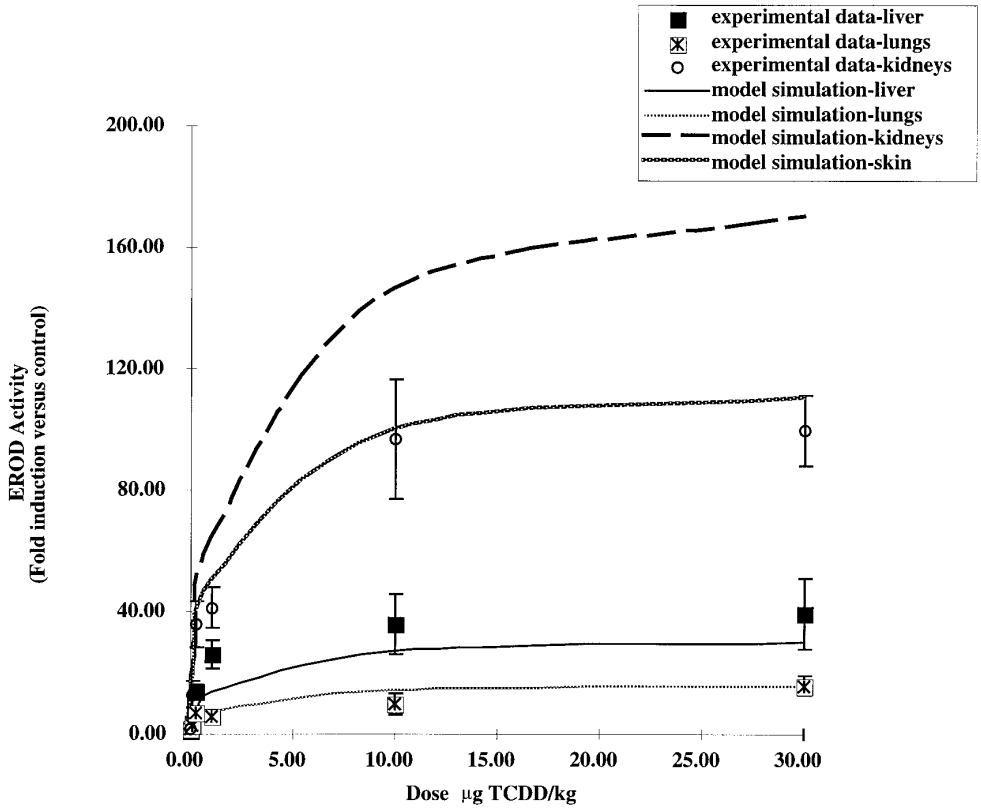

FIG. 8. Dose-dependent effects of TCDD on EROD activity in the liver, lungs, kidneys, and skin of female Sprague–Dawley rats with BBPD model simulation. EROD activity was quantitated spectrofluorimetrically as described (DeVito *et al.,* 1996). EROD activity is expressed as fold induction compared to control animals. All symbols were obtained from TCDD-treated animals as described in Materials and Methods. Solid and broken lines were derived from the BBPD model simulation of the experimental data. ■, EROD activity in liver; ○, EROD activity in kidneys; x, EROD activity in lungs. Data are presented as mean ± SD (n = 4–5).

1) was similar to the maximum hepatic EROD induction rate observed by van Birgelen and coworkers (1996) using female Sprague–Dawley rats. The present BBPD model assumes that both the induction of CYP1A2 and CYP1A1 share a similar mechanism of TCDD-induced gene expression. The BBPD model simulations (Figs. 2–5) well represent the time-dependent effects of TCDD on hepatic CYP1A1/CYP1A2-dependent enzymatic activities (or CYP1A1/CYP1A2 protein concentration).

The model obtained from the time-course studies were applied to describe the dose-dependent increase in TCDD-induced cytochrome P450 protein expression and associated enzyme activities in the liver of female Sprague–Dawley rats at 3 days following a single exposure to TCDD (0.01–30.0μg TCDD/kg). Figure 6 shows that the shape of the model simulation well presented the dose-dependent change in hepatic CYP1A1 protein expression by TCDD. However, the BBPD model underpredicted TCDD-induced CYP1A1 protein expression in the liver of rats treated with 1 μg TCDD/kg (Fig. 6). In addition, the BBPD model underpredicted the hepatic TCDD-induced EROD activity (Fig. 8). Since EROD activity is a linear biomarker of CYP1A1 protein expression, the linear coefficient between EROD activity and CYP1A1 obtained from time-course and dose-dependent studies should be the same. However, the underprediction in Fig. 8 indicates that the linear coefficient from the time-course and dose-response studies are different. These inconsistencies between experiments may be due to differences in sample preparation as observed in previous studies from our laboratory (DeVito *et al.,* 1994a; van Birgelen *et al.,* 1996). For example, the samples from the dose-response study were homogenized prior to freezing. In contrast, the samples from the time-course study were frozen as whole tissues prior to homogenization. Previous studies have illustrated a 20–40% decrease in cytochrome P450 enzymes as a result of freezing the liver prior to homogenization (Pearce *et al.,* 1996). In addition, recent studies have suggested that cytochrome P450 immunoreactive protein is detected with or without thawing prior to homogenization, but catalytic activity is decreased dramatically by thawing of the liver (Yamazaki *et al.,* 1997). The hepatic EROD activity and CYP1A1 protein concentration obtained from the control animals in both studies support the hypothesis above. For example, constitutive hepatic EROD activity for the time-course studies was 343 pmol/min/mg microsomal protein. In contrast,

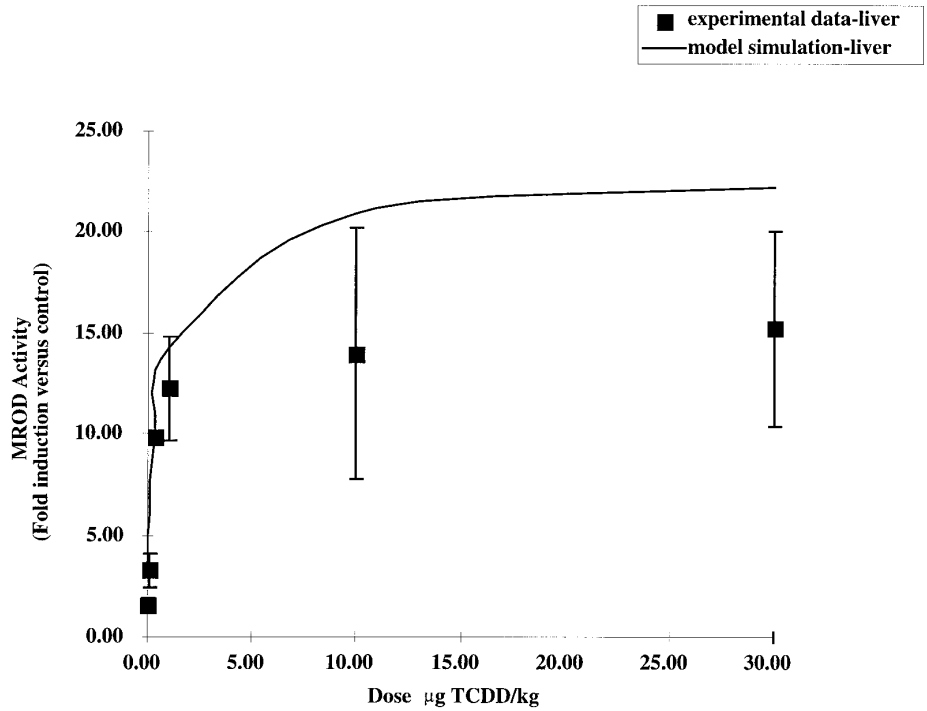

FIG. 9. Dose-dependent effects of TCDD on MROD activity in the liver of female Sprague–Dawley rats with BBPD model simulation. MROD activity was quantitated spectrofluorimetrically as described (DeVito *et al.,* 1996). MROD activity is expressed as fold induction compared to control animals. All symbols were obtained from TCDD-treated animals as described in Materials and Methods. The solid line was derived from the BBPD model simulation of the experimental data. ■, MROD activity in liver. Data are presented as mean ± SD (n = 4–5).

the constitutive hepatic EROD activity for the dose-dependent studies was higher (490 pmol/min/mg microsomal protein).[5] However, in both studies the control CYP1A1 protein concentration were the same (0.02 optical density units/μg microsomal protein). This demonstrates that the differences in sample preparation between the two studies may have influenced hepatic EROD activity without any apparent change in relative hepatic CYP1A1 protein concentration. Therefore, the model developed on time-course data accurately predicts the dose-dependent effect of TCDD on hepatic CYP1A1 protein expression (Fig. 6) but underpredicts the hepatic EROD activity (Fig. 8), possibly due to differences in sample preparation. However, other factors such as genetic variability in the outbred Sprague–Dawley rat population (Hull *et al.,* 1983) and seasonal changes in drug-metabolizing enzyme activity (Robinson *et al.,* 1974), which were not addressed in this study, may have contributed, in part, to the slight differences obtained in the hepatic EROD activity obtained in control animal populations.

Roth *et al.* (1994) predicted the induction of CYP1A2 using specific rates for synthesis and degradation for this enzyme (Parkinson *et al.,* 1983; Shiraki and Guengerich, 1984). In this study, the model obtained from the time-course studies was then applied to predict the dose-dependent change in TCDD-induced CYP1A2 protein expression and MROD activity in the liver of female Sprague–Dawley rats at 3 days following a single exposure to TCDD (0.01–30.0 μg TCDD/kg). The shape of the model simulations represent both the dose-dependent effects of TCDD on CYP1A2 protein expression (Fig. 7) and MROD activity (Fig. 9). However, the BBPD model underpredicted the CYP1A2 protein expression obtained in the 35-day TCDD-treatment group (Fig. 3) and MROD activity (Fig. 5). The underprediction of both hepatic TCDD-induced CYP1A2 protein expression and MROD activity may be due to the interaction of TCDD-induced CYP1A2 protein with TCDD resulting in an inactivation of CYP1A2 (Fig. 1) and subsequent loss of immunodetectable CYP1A2 protein and measurable MROD activity. Another reason for the underprediction of both TCDD-induced CYP1A2 protein expression and MROD activity may be due to differences in sample preparation (DeVito *et al.,* 1994a; van Birgelen *et al.,* 1996) as discussed above. For example, constitutive hepatic MROD activity and CYP1A2 protein concentration for the time-course studies were 74 pmol/min/mg microsomal protein and 0.03 optical density units/μg microsomal protein, respectively. In contrast, the constitutive hepatic MROD activity and CYP1A2 protein concentration for the dose-dependent studies were higher (171 pmol/min/mg microsomal protein and 0.08 optical density units/μg microsomal protein, respectively). This demonstrated

[5] EROD activities from control animals obtained from the different hepatic tissue preparations were not significantly different as determined by ANOVA.

that the differences in sample preparation between the two studies would influence both MROD activity and CYP1A2 protein concentration. Therefore, the model developed on time-course data underpredicts both the dose-dependent effect of TCDD on CYP1A2 protein expression (Figure 7) and MROD activity (Fig. 9) in the liver possibly due to differences in sample preparation between the time-course and dose-dependent studies. However, other factors, as described above, may have also contributed to the slight differences observed.

TCDD induces a broad spectrum of sex-, strain-, age-, tissue-, and species-specific toxic effects, which include a wasting syndrome, thymic atrophy, immunotoxicity, hepatotoxicity, pulmonary toxicity, chloracne and related dermal toxicity, teratogenicity, reproductive toxicity, and carcinogenicity (reviewed in Safe, 1986; Birnbaum, 1994a; Pohjanvirta and Tuomisto, 1994; Van den Berg *et al.,* 1994). For example, dermal treatment of female hairless mice (HRS/J *hr/hr*) with the *N*-methyl-*N'*-nitro-*N*-nitrosoguanidine (MNNG) and with TCDD (2.5–10.0 ng TCDD/mouse/dose) as the promoter resulted in the induction of squamous cell papillomas (Hebert *et al.,* 1990). In addition, promotion of *N*-nitrosodimethylamine (NDMA)- or *N*-nitrosodiethylamine-initiated lung tumors in male mice (Beebe *et al.,* 1995) and liver tumors in female rats (Pitot *et al.,* 1980) exposed to TCDD has been demonstrated. These data suggest that in experimental animals, TCDD is classified as a multi-site, sex- and species-specific complete carcinogen (DeVito and Birnbaum, 1994b). However, TCDD also induces many phase I drug metabolizing enzymes (reviewed in Whitlock *et al.,* 1996; Whitlock, 1993), including CYP1A1, CYP1A2 and CYP1B1 in multiple tissues (Diliberto *et al.,* 1995; Santostefano *et al.,* 1996, 1997b). For example, TCDD treatment results in the dose-dependent increase in EROD activity in rat liver, lungs, and kidneys (Santostefano *et al.,* 1996) and liver, lungs and skin of mice (Diliberto *et al.,* 1995). However, previous pharmacodynamic models for TCDD have focused on TCDD-induced responses in liver (Leung *et al.,* 1988, 1990a; Andersen and Greenlee, 1991; Andersen *et al.,* 1993; Buckley-Kedderis *et al.,* 1993; Kohn *et al.,* 1993; Roth *et al.,* 1994). In this paper the time-dependent effects of TCDD on CYP1A1-associated EROD activity was determined in multiple target tissues (lungs, skin and kidneys) for TCDD-mediated toxic and biochemical responses and analyzed by a BBPD model. This BBPD model accurately describes the time course of CYP1A1 protein expression and EROD activity in the lungs, skin, and kidneys (Fig. 4). The BBPD model also illustrated that EROD activity could be an appropriate marker for CYP1A1 protein expression as observed in previous studies (Santostefano *et al.,* 1996 and references therein). The shape of the curves in Figs. 2 and 4 supports the hypothesis that a similar time-dependent mechanism of TCDD-induced CYP1A1 protein expression and associated EROD activity occurs in multiple tissues (Diliberto *et al.,* 1995; Santostefano *et al.,* 1996, 1997b). This data suggests that parameter estimation in this study (Table 1) accurately described the AhR-mediated mechanism (Fig. 1) of TCDD on protein expression and enzymatic activities in multiple tissues.

The BBPD model obtained from the time-course studies well described the dose-dependent change in TCDD-induced cytochrome P450 protein expression and associated enzyme activities in the lungs and kidneys of female Sprague–Dawley rats at 3 days following a single exposure to TCDD (0.01–30.0 μg TCDD/kg). In comparison to the BBPD model slight underprediction of hepatic EROD activity, Fig. 6 shows that the BBPD model slightly overpredicted the dose-dependent effects of TCDD on EROD activity in the lungs and kidneys. The constitutive EROD activities for the time-course studies were 6 and 11 pmol/min/mg microsomal protein, for the kidneys and lungs, respectively, and the constitutive EROD activities for the dose-dependent studies in extrahepatic tissues were lower (kidneys are 2 and lungs are 3 pmol/min/mg microsomal protein). These differences in constitutive EROD activity in extrahepatic tissues, as compared to the liver obtained from the different sample preparations, resulted in the BBPD model over predicting the dose-dependent effects of TCDD on EROD activity in extrahepatic tissues (Fig. 8). Previous studies from our laboratory (DeVito *et al.,* 1994a; van Birgelen *et al.,* 1996) also observed a slight change in EROD activity in extrahepatic tissues as a result of differences in tissue sample preparations. The BBPD model also suggested that TCDD would cause a similar dose-dependent increase in EROD activity in the skin as in the liver, kidneys, and lungs (Fig. 8) indicating that a similar time- and dose-dependent mechanism action of TCDD-induced EROD activity occurs in multiple tissues (Diliberto *et al.,* 1995; Santostefano *et al.,* 1996, 1997b). Furthermore, the model was utilized to simulate the dose-dependent effects of TCDD on CYP1A1 protein expression in the lungs, kidneys, and skin. The BBPD model illustrated that TCDD would cause a similar dose-dependent increase in CYP1A1 protein expression in the lungs, kidneys, and skin as in the liver (Fig. 6), suggesting that a similar time- and dose-dependent mechanism action of both TCDD-induced CYP1A1 protein expression and associated EROD activity occurs in multiple tissues (Diliberto *et al.,* 1995; Santostefano *et al.,* 1996, 1997b). Whether the BBPD model overpredicts the relative CYP1A1 concentration in extrahepatic tissues may depend upon the influence of sample preparation on CYP1A1 protein expression in extrahepatic tissues. In addition, other factors such as genetic variability in the Sprague–Dawley rat population (Hull *et al.,* 1983) and seasonal changes (Robinson *et al.,* 1974), which were not addressed in this study, may have contributed, in part, to the slight differences obtained in animal populations.

This BBPD model quantitatively describes for the first time the time-course relationship between TCDD-induced CYP1A1/CYP1A2 protein expression and associated enzyme activities and tissue disposition in multiple tissues of female Sprague–Dawley rats. In addition, this BBPD model differs from other models by validating the BBPD model and parameters obtained from the time-course studies in multiple tissues by

predicting the dose-dependent effects of TCDD on cytochrome P450 protein expression and associated enzyme activities in the multiple tissues of female Sprague–Dawley rats at 3 days following a single exposure to TCDD (0.01–30.0 μg TCDD/kg). Moreover, this BBPD model demonstrates the importance of experimental design and sample preparation for a quantitative description of the time- and dose-dependent effects of TCDD on cytochrome P450 gene expression and associated enzymatic activities. However, further validation of this simultaneous PBPK and BBPD model across different routes of exposure, sexes of rats and species needs to be examined.

The overall goal of the development of this simultaneous PBPK and BBPD model is to quantitatively link the concentration of the chemical at the site of action to chemical-induced gene expression based upon the actual physiology of the organism and physiochemical properties and mechanism of action of the chemical of interest. Previously, Wang and coworkers (1997a) developed and validated a PBPK model to describe the time- and dose-dependent tissue distribution of TCDD in female Sprague–Dawley rats. This PBPK model was further validated using different routes of exposure (oral and iv), sexes of rats (female and male), and species (rats and mice) (Wang *et al.*, 1997b). In our current study, we extended the previous pharmacokinetic models by determining the parameter values based on time course of CYP1A1 and CYP1A2 responses in multiple tissues after acute exposure to TCDD using a simultaneous PBPK and BBPD model and then validated the model with data obtained from dose-dependent studies. The development of accurate mechanistically based pharmacokinetic and pharmacodynamic models and further validation of these models across other classes of environmental contaminants with a similar mechanism of action will increase the confidence in the use of these models in approaches for human risk assessment as related to environmental exposure and potential for adverse health risks.

ACKNOWLEDGMENTS

This project could not have been accomplished without the technical assistance of Janet J. Diliberto at the U.S. Environmental Protection Agency (USEPA), Research Triangle Park (RTP), NC. In addition, the authors thank Dr. Marina V. Evans (USEPA, RTP, NC), Dr. Keith Ward (Curriculum in Toxicology, University of North Carolina at Chapel Hill, Chapel Hill, NC), and Mr. Christopher R. Eklund (USEPA, RTP, NC) for reviewing the manuscript prior to submission.

REFERENCES

Andersen, M. E., and Greenlee, W. F. (1991). Biological determinants of TCDD pharmacokinetics and their relationship to a biological-based risk assessment. In *Biological Basis for Risk Assessment of Dioxins and Related Compounds* (M. Gallo, R. J. Scheuplein, and K. A. Van Der Heijden, Eds.), pp. 291–307. Cold Spring Harbor Laboratory Press, Cold Spring Harbor, NY.

Andersen, M. E., Mills, J. J., Gargas, M. L., Kedderis, L., Birnbaum, L. S., Neubert, D., and Greenlee, W. F. (1993). Modeling receptor-mediated processes with dioxin: Implications for pharmacokinetics and risk assessment. *Risk Anal.* **13,** 25–36.

Beebe, L. E., Anver, M. R., Iggs, C. W., Fornwald, L. W., and Anderson, L. M. (1995). Promotion of N-nitrosodimethylamine-initiated mouse lung tumors following single or multiple low dose exposure to 2,3,7,8-tetrachlorodibenzo-*p*-dioxin. *Carcinogenesis* **16,** 1345–1349.

Birnbaum, L. S. (1994a). Evidence for the role of the Ah receptor in response to dioxin. In *Receptor-Mediated Biological Processes: Implications for Evaluating Carcinogenesis* (H. L. Spitzer, T. J. Slaga, W. F. Greenlee, and M. McClain, Eds.), pp. 139–154. Wiley-Liss, New York.

Birnbaum, L. S. (1994b). The mechanism of dioxin toxicity: Relationship to risk assessment. *Environ. Health Perspect.* **102 (Suppl. 9),** 157–167.

Bradford, M. M. (1976). A rapid and sensitive method for the quantitation of microgram quantities of protein utilizing the principle of protein-dye binding. *Anal. Biochem.* **72,** 248–254.

Buckley, L. A. (1995). Biologically based model of dioxin pharmacokinetics. *Toxicology* **102,** 125–131.

Buckley-Kedderis, L., Diliberto, J. J., Linko, P., Goldstein, J. A., and Birnbaum, L. S. (1991). Disposition of 2,3,7,8-tetrabromodibenzo-*p*-dioxin and 2,3,7,8-tetrachlorodibenzo-*p*-dioxin in the rat: Biliary excretion and induction of cytochromes CYP1A1 and CYP1A2. *Toxicol. Appl. Pharmacol.* **111,** 163–172.

Buckley-Kedderis, L. B., Mills, J. J., Andersen, M. E., and Birnbaum, L. S. (1993). A physiologically based pharmacokinetic model for 2,3,7,8-tetrabromodibenzo-*p*-dioxin (TBDD) in the rat: Tissue distribution and CYP1A induction. *Toxicol. Appl. Pharmacol.* **121,** 87–98.

Chaloupka, K., Steinberg, M., Santostefano, M., Rodriquez, L. V., Goldstein, L., and Safe, S. (1995). Induction of Cyp1a-1 and Cypla-2 gene expression by a reconstituted mixture of polynuclear aromatic hydrocarbons in B6C3F1 mice. *Chem.–Biol. Interact.* **96,** 207–221.

Chen, H. S., and Perdew, G. H. (1994). Subunit composition of the heteromeric cytosolic aryl hydrocarbon receptor complex. *J. Biol. Chem.* **269,** 27554–27558.

Cuthill, S., Wilhelmsson, A., and Poellinger, L. (1991). Role of the ligand in intracellular receptor function: Receptor affinity determines activation *in vitro* of the latent dioxin receptor to a DNA-binding form. *Mol. Cell. Biol.* **11,** 401–411.

David, H. T. (1978). Goodness of fit. In *International Encyclopedia of Statistics* (W. M. Kruskal, and J. M. Tanur, Eds.), pp. 399–409. The Free Press, New York.

Dayneka, N. L., Garg, V., and Jusko, W. J. (1993). Comparison of four basic models of indirect pharmacodynamic response. *J. Pharmacol. Biopharmacol.* **21,** 457–478.

Denison, M. S., Okey, A. B., Hamilton, J. W., Bloom, S. E., and Wilkinson, C. F. (1986a). Ah receptor for 2,3,7,8-tetrachlorodibenzo-*p*-dioxin: Ontogeny in chick embryo liver. *J. Biochem. Toxicol.* **1,** 39–46.

Denison, M. S., Wilkinson, C. F., and Okey, A. B., (1986b). Ah receptor for 2,3,7,8-tetrachlorodibenzo-*p*-dioxin: Comparative studies in mammalian and non-mammalian species. *Chemosphere* **15,** 1665–1672.

Denison, M. S., Fisher, J. M., and Whitlock, J. P., Jr. (1988a). The DNA recognition site for the dioxin-Ah receptor complex. *J. Biol. Chem.* **263,** 17221–17224.

Denison, M. S., Fisher, J. M., and Whitlock, J. P., Jr. (1988b). Inducible, receptor-dependent protein-DNA interaction at a dioxin-responsive transcriptional enhancer. *Proc. Natl. Acad. Sci. USA* **85,** 2528–2532.

Denison, M. S., and Yao, E. F. (1991). Characterization of the interaction of transformed rat hepatic cytosolic Ah receptor with a dioxin responsive transcriptional enhancer. *Arch. Biochem. Biophys.* **284,** 158–166.

DeVito, M. J., Beebe, L. E., Menache, M., and Birnbaum, L. S. (1996). Relationship between CYP1A enzyme activities and protein levels in rats

treated with 2,3,7,8-tetrachlorodibenzo-*p*-dioxin. *J. Toxicol. Environ. Health* **47,** 379–394.

DeVito, M. J., Ma, X., Babish, J. G., Menache, M., and Birnbaum, L. S. (1994a). Dose-response relationships in mice following subchronic exposure to 2,3,7,8-tetrachlorodibenzo-*p*-dioxin: CYP1A1, CYP1A2, estrogen receptor, and protein tyrosine phosphorylation. *Toxicol. Appl. Pharmacol.* **124,** 82–90.

DeVito, M. J., and Birnbaum, L. S. (1994b). Toxicology of dioxins and related chemicals. In *Dioxins and Health* (A. Schecter, Ed.), pp. 139–162. Plenum Press, New York.

Diliberto, J. J., Akubue, P. I., Luebke, R. W., and Birnbaum, L. S. (1995). Dose-response relationships of tissue distribution and induction of CYP1A1 and CYP1A2 enzymatic activities following acute exposure to 2,3,7,8-tetrachlorodibenzo-*p*-dioxin in mice. *Toxicol. Appl. Pharmacol.* **130,** 197–208.

Diliberto, J. J., Burgin, D., and Birnbaum, L. S. (1997). Role of CYP1A2 in hepatic sequestration of dioxin: Studies using CYP1A2 knock-out mice. *Biochem. Biophys. Res. Commun.* **236,** 431–433.

Elferink, C. J., Gasiewicz, T. A., and Whitlock, J. P., Jr. (1990). Protein-DNA interactions at a dioxin-responsive enhancer: Evidence that the transformed Ah receptor is heteromeric. *J. Biol. Chem.* **265,** 20708–20712.

Favreau, L. V., and Pickett, C. B. (1991). Transcriptional regulation of the rat NAD(P)H:quinone reductase gene. *J. Biol. Chem.* **266,** 4556–4561.

Fujisawa-Sehara, A., Sogawa, K., Yamane, M., and Fujii-Kuriyama, Y. (1986). Regulatory DNA elements localized remotely upstream from the drug-metabolizing cytochrome P-450c gene. *Nucleic Acids Res.* **14,** 1465–1477.

Gonzalez, F. J., and Nebert, D. W. (1985). Autoregulation plus upstream positive and negative control regions associated with transcriptional activation of the mouse cytochrome P1-450 gene. *Nucleic Acids Res.* **13,** 7269–7288.

Guengerich, F. P. (1990). Enzymatic oxidation of xenobiotic chemicals. *CRC Crit. Rev. Biochem. Mol. Biol.* **25,** 97–153.

Hankinson, O. (1995). The aryl hydrocarbon receptor complex. *Annu. Rev. Pharmacol. Toxicol.* **35,** 307–340.

Hebert, C. E., Harris, M. W., Elwell, M. R., and Birnbaum, L. S. (1990). Relative toxicity and tumor-promoting ability of 2,3,7,8-tetrachlorodibenzo-*p*-dioxin (TCDD), 2,3,4,7,8-pentachlorodibenzofuran (PCDF), and 1,2,3,4,7,8-hexachlorodibenzofuran (HCDF) in hairless mice. *Toxicol. Appl. Pharmacol.* **102,** 362–377.

Hoffman, E. C., Reyes, H., Chu, F.-F., Sander, F., Conley, L. H., Brooks, B. A., and Hankinson, O. (1991). Cloning of a factor required for activity of the Ah (dioxin) receptor. *Science* **252,** 954–958.

Hull, B. E., Sher, S. E., Rosen, S., Church, D., and Bell, E. (1983). Structural integration of skin equivalents grafted to Lewis and Sprague–Dawley rats. *J. Invest. Dermatol.* **81,** 429–435.

Israel, D. I., Estolano, M. G., Galeazzi, D. R., and Whitlock, J. P., Jr. (1985). Superinduction of cytochrome P1-450 gene transcription by inhibition of protein synthesis. *J. Biol. Chem.* **260,** 5648–5653.

King, F. G., Dedrick, R. L., Collins, J. M., Matthews, H. B., and Birnbaum, L. S. (1983). A physiological model for the pharmacokinetics of 2,3,7,8-tetrachlorodibenzofuran in several species. *Toxicol. Appl. Pharmacol.* **67,** 390–400.

Kohn, M. C., Lucier, G. W., Clark, G. C., Sewall, C., Tritscher, A. M., and Portier, C. J. (1993). A mechanistic model of effects of dioxin on gene expression in the rat liver. *Toxicol. Appl. Pharmacol.* **120,** 138–154.

Kohn, M. C., Sewall, C. H., Lucier, G. W., and Portier, C. J. (1996). A mechanistic model of effects of dioxin on thyroid hormones in the rat. *Toxicol. Appl. Pharmacol.* **165,** 29–48.

Laemmli, U. K. (1970). Cleavage of structural proteins during the assembly of bacteriophage T4. *Nature* **277,** 680–685.

Legraverend, C., Hannah, R. T., Eisen, H. J., Owens, I. S., Nebert, D. W., and Hankinson, O. (1982). Regulatory gene product of the Ah locus. Characterization of receptor mutants among mouse hepatoma clones. *J. Biol. Chem.* **257,** 6402–6407.

Leung, H. W., Ku, R. H., Paustenbach, D. J., and Andersen, M. E. (1988). A physiological-based pharmacokinetic model for 2,3,7,8-tetrachlorodibenzo-*p*-dioxin in C57BL/6J and DBA/2J mice. *Toxicol. Lett.* **42,** 15–28.

Leung, H. W., Paustenbach, D. J., Murray, F. J., and Andersen, M. E. (1990a). A physiological pharmacokinetic description of the tissue distribution and enzyme-inducing properties of 2,3,7,8-tetrachlorodibenzo-*p*-dioxin in the rat. *Toxicol. Appl. Pharmacol.* **103,** 399–410.

Leung, H. W., Poland, A., Paustenbach, D. J., Murray, F. J., and Andersen, M. E. (1990b). Pharmacokinetics of [^{125}I]-2-iodo,3,7,8-trichlorodibenzo-*p*-dioxin mice: Analysis with a physiological modeling approach. *Fundam. Appl. Pharmacol.* **103,** 411–419.

Okey, A. B., Bondy, G. P., Mason, M. E., Nebert, D. W., Forster-Gibson, C. J., and Dufresne, M. J., (1980). Temperature-dependent cytosol-to-nucleus translocation of the Ah receptor for 2,3,7,8-tetrachlorodibenzo-*p*-dioxin in continuous cell culture. *J. Biol. Chem.* **255,** 11415–11422.

Parkinson, A., Thomas, P. E., Ryan, D. E., Reik, L. M., Safe, S. H., Robertson, L. W., and Levin, W. (1983). Differential time course of induction of rat liver microsomal cytochrome P-450 isozymes and epoxide hydrolase by Aroclor 1254. *Arch. Biochem. Biophys.* **225,** 203–215.

Pearce, R. E., McIntyre, C. J., Madan, A., Sanzgiri, U., Draper, A. J., Bullock, P. L., Cook, D. C., Burton, L. A., Latham, J., Nevins, C., and Parkinson, A. (1996). Effects of freezing, thawing, and storing human liver microsomes on cytochrome P450 activity. *Arch. Biochem. Biophys.* **331,** 145–169.

Pitot, H. C., Goldsworthy, T., Campbell, H. A., and Poland, A. (1980). Quantitative evaluation of the promotion of 2,3,7,8-tetrachlorodibenzo-*p*-dioxin of hepatocarcingenesis from diethylnitrosamine. *Cancer Res.* **40,** 3616–3620.

Pohjanvirta, R., and Tuomisto, J. (1994). Short-term toxicity of 2,3,7,8-tetrachlorodibenzo-*p*-dioxin in laboratory animals: Effects, mechanisms, and animal models. *Pharmacol. Rev.* **46,** 483–549.

Pohl, R. A., and Fouts, J. R. (1980). A rapid method for assaying the metabolism of 7-ethoxyresorufin by microsomal subcellular fractions. *Anal. Biochem.* **107,** 150–155.

Poland, A., and Glover, E. (1974). Comparison of 2,3,7,8-tetrachlorodibenzo-*p*-dioxin, a potent inducer of aryl hydrocarbon hydroxylase, with 3-methylcholanthrene. *Mol. Pharmacol.* **10,** 349–359.

Poland, A., Teitelbaum, P., and Glover, E. (1989a). [^{125}I]2-iodo-3,7,8-trichlorodibenzo-*p*-dioxin-binding species in mouse liver induced by agonists for the Ah receptor: Characterization and identification. *Molec. Pharmacol.* **36,** 113–120.

Poland, A., Teitelbaum, P., Glover, E., and Kende, A. (1989b). Stimulation of *in vivo* hepatic uptake and *in vitro* hepatic binding of [^{125}I]2-iodo-3,7,8-trichlorodibenzo-*p*-dioxin by the administration of agonists for the Ah receptor. *Mol. Pharmacol.* **36,** 121–127.

Portier, C., and Hoel, D. (1983). Optimal design of the chronic animal bioassay. *J. Toxicol. Environ. Health* **12,** 1–9.

Portier, C. J., and Hoel, D. G. (1984). Design of animal carcinogenicity studies for goodness-of-fit of multistage models. *Fundam. Appl. Toxicol.* **4,** 949–959.

Portier, C., Tritscher, A., Kohn, M., Sewall, C., Clark, G., Elder, L., Hoel, D., and Lucier, G. (1993). Ligand/receptor binding for 2,3,7,8-TCDD: Implications for risk assessment. *Fundam. Appl. Toxicol.* **20,** 48–56.

Quattrochi, L. C., Vu, T., and Tukey, R. H. (1994). The human CYP1A2 gene and induction by 3-methylcholanthrene. *J. Biol. Chem.* **269,** 6949–6954.

Robinson, J. R., Considine, N., and Nebert, D. W. (1974). Genetic expression of aryl hydroxylase induction. Evidence for the involvement of other genetic loci. *J. Biol. Chem.* **249,** 5851–5859.

Roth, W. L., Ernst, S., Weber, L. W. D., Kerecsen, L., and Rozman, K. K. (1994). A pharmacodynamically responsive model of 2,3,7,8-tetrachlorodibenzo-*p*-dioxin (TCDD) transfer between liver and fat at low and high doses. *Toxicol. Appl. Pharmacol.* **127,** 151–162.

Rushmore, T. H., and Pickett, C. B. (1990). Transcriptional regulation of the rat glutathione S-transferase Ya subunit gene: Characterization of a xenobiotic-responsive element controlling inducible expression by phenolic antioxidants. *J. Biol. Chem.* **265,** 14648–14653.

Safe, S. H. (1986). Comparative toxicology and mechanism of action of polychlorinated dibenzo-*p*-dioxins and dibenzofurans. *Annu. Rev. Pharmacol. Toxicol.* **26,** 371–379.

Santostefano, M. J., Johnson, K. L., Whisnant, N. A., Richardson, V. M., DeVito, M. J., Diliberto, J. J., and Birnbaum, L. S. (1996). Subcellular localization of TCDD differs between the liver, lungs and kidneys after acute and subchronic exposure: Species/dose comparisons and possible mechanism. *Fundam. Appl. Toxicol.* **34,** 265–275.

Santostefano, M. J., Diliberto, J. J., and Birnbaum, L. S. (1997a). CYP1A2 knockout mice: Decreased hepatic microsomal localization of TCDD. In *Organohanlogen Compounds* (R. Hites, Ed.), pp. 19–24. Indianapolis, IN.

Santostefano, M. J., Ross, D. G., Savas, U., Jefocate, C. R., and Birnbaum, L. S. (1997b). Differential hepatic regulation of rat CYP1B1, CYP1A1 and CYP1A2 proteins by TCDD. *Biochem. Biophys. Res. Commun.* **233,** 20–24.

Savas, U., Bhattacharyya, K. K., Christou, M., Alexander, D. L., and Jeffcoate, C. R., (1994). Mouse cytochrome P-450EF, representative of a new 1B subfamily of the cytochrome P-450s. *J. Biol. Chem.* **269,** 14905–14911.

Shiraki, H., and Guengerich, F. P. (1984). Turnover of membrane proteins: Kinetics of induction and degradation of several forms of rat liver microsomal cytochrome P-450, NADPH-cytochrome P-450 reductase, and epoxide hydrolase. *Arch. Biochem. Biophys.* **15,** 86–96.

Telakowski-Hopkins, C. A., King, R. G., and Pickett, C. B. (1988). Glutathione S-transferase Ya subunit gene: Identification of regulatory elements required for basal level and inducible expression. *Proc. Natl. Acad. Sci. USA* **85,** 1000–1004.

Towbin, H., Staehelin, T., and Gordon, J. (1979). Electrophoretic transfer of proteins from polyacrylamide gels to nitrocellulose sheets: Procedure and some applications. *Proc. Natl. Acad. Sci. USA* **76,** 4350–4354.

Tritscher, A. M., Clark, G. C., and Lucier, G. W. (1994). Dose-response effects of dioxins. In *Dioxins and Health* (A. Schecter, Ed.), pp. 227–250. Plenum Press, New York.

Tritscher, A. M., Goldstein, J. A., Portier, C. J., McCoy, Z., Clark, G. C., and Lucier, G. W. (1992). Dose-response relationships for chronic exposure to 2,3,7,8-tetrachlorodibenzo-*p*-dioxin in a rat tumor promotion model: Quantification and immunolocalization of CYP1A1 and CYP1A2 in the liver. *Cancer Res.* **52,** 3436–3442.

van Birgelen, A. P. J. M., DeVito, M. J., and Birnbaum, L. S. (1996). Toxic equivalency factors derived from cytochrome P450 induction in mice are predictive for cytochrome P450 induction after subchronic exposure to mixtures of PCDDS, PCDFs, and PCBs in female B6C3F1 mice and Sprague–Dawley rats. In *Organohanlogen Compounds* (R. Hites, Ed.), pp. 251–256. Amsterdam, The Netherlands.

Van den Berg, M., De Jongh, J., Poiger, H., and Olson, J. R. (1994). The toxicokinetics and metabolism of polychlorinated dibenzo-*p*-dioxin (PCDDs), and dibenzofurans (PCDFs) and their relevance for toxicity. *Crit. Rev. Toxicol.* **24,** 1–74.

Voorman, R., and Aust, S. D. (1987). Specific binding of polyhalogenated aromatic hydrocarbon inducers of cytochrome P-450d to the cytochrome and inhibition of its estradiol 2-hydroxylase activity. *Toxicol. Appl. Pharmacol.* **90,** 69–78.

Voorman, R., and Aust, S. D. (1989). TCDD (2,3,7,8-tetrachlorodibenzo-*p*-dioxin) is a tight binding inhibitor of cytochrome P-450d. *J. Biochem. Toxicol.* **4,** 105–109.

Wang, X., Santostefano, M. J., Evans, M. V., Richardson, V. M., Diliberto, J. J., and Birnbaum, L. S. (1997a). Determination of parameters responsible for pharmacokinetic behavior of TCDD in female Sprague-Dawley rats. *Toxicol. Appl. Pharmacol.* **147,** 151–168.

Wang, X., Santostefano, M. J., DeVito, M. J., and Birnbaum, L. S. (1997b). Extrapolation of a previous PBPK model for TCDD across routes of exposure, gender, and from rats to mice. In *Organohanlogen Compounds* (R. Hites, Ed.) pp. 38–42. Indianapolis, IN.

Weber, L. W. D., Ernst, S. W., Stahl, B. U., and Rozman, K. (1993). Tissue distribution and toxicokinetics of 2,3,7,8-tetrachlorodibenzo-*p*-dioxin in rats after intravenous injection. *Fundam. Appl. Toxicol.* **21,** 523–534.

Whitelaw, M., Pongratz, I., Wilhelmsson, A., Gustafsson, J.-A., and Poellinger, L. (1993). Ligand-dependent recruitment of the Arnt coregulator determines DNA recognition by the dioxin receptor. *Mol. Cell. Biol.* **13,** 2504–2514.

Whitlock, J. P., Jr. (1993). Mechanistic aspects of dioxin action. *Chem. Res. Toxicol.* **6,** 754–763.

Whitlock, J. P., Jr., Okino, S. T., Ko, H. P., Clarke-Katzenberg, R., Ma, Q., and Li, H. (1996). Induction of cytochrome P-4501A1: A model for analyzing mammalian gene transcription. *FASEB J.* **10,** 809–818.

Yamazaki, H., Inoue, K., Turvy, C. G., Guengerich, F. P., and T., S. (1997). Effects of freezing, thawing, and storage of human liver samples on the microsomal contents and activities of cytochrome P450 enzymes. *Drug Metab. Dispos.* **25,** 168–174.